

# GREEN'S FUNCTION METHOD FOR ELECTRON DIFFRACTION AND BAND STRUCTURE PROBLEMS

By

VIBHAKAR VASANTRAO BHOKARE

Phy  
1973  
D  
BHO  
GRE

TH  
PHY/1973/D  
8469g



DEPARTMENT OF PHYSICS  
INDIAN INSTITUTE OF TECHNOLOGY KANPUR  
DECEMBER, 1973

PhD  
30227

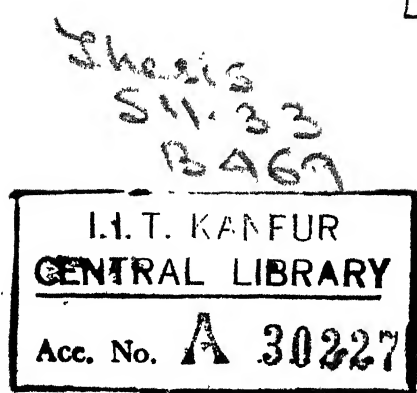
# **GREEN'S FUNCTION METHOD FOR ELECTRON DIFFRACTION AND BAND STRUCTURE PROBLEMS**

A Thesis Submitted  
In Partial Fulfilment of the Requirements  
for the Degree of  
**DOCTOR OF PHILOSOPHY**

By  
**VIBHAKAR VASANTRAO BHOKARE**

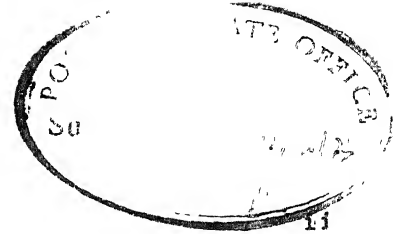
to the

**DEPARTMENT OF PHYSICS**  
**INDIAN INSTITUTE OF TECHNOLOGY KANPUR**  
**DECEMBER, 1973**



13 SEP 1974

PHY-1973-D - BHO - GRE



## C E R T I F I C A T E

This is to certify that the work presented in this thesis by  
Vibhakar Vasantrao Bhokare was performed under my supervision  
at Indian Institute of Technology, Kanpur and that it is original  
and has not been submitted elsewhere for a degree.

*M. Yussouff*

Dr. M. Yussouff

24.10.1974

Ph.D.	Thesis
for	the
Year	(1974)
to	be
submitted	to the
Institute	Indian Institute of Technology, Kanpur
Dated:	31/8/74

INSTITUT FÜR THEORETISCHE PHYSIK  
DER UNIVERSITÄT ZU KÖLN  
5 KÖLN 41 · ZÜLPICHER STR. 77

and

on leave of Absence from  
Indian Institute of Technology  
Kanpur - 16 (U.P.) India

#### ACKNOWLEDGEMENTS

The author is indebted to Dr. M. Yussouff for suggesting the problem and for his guidance and continuous encouragement throughout the course of the present work. The author is also thankful to Professor R. P. Singh and Dr. M. M. Pant for helpful discussions.

The author would like to express his gratitude to Dr. Sushma Tewari for some computer programmes and to Mr. Ashok Kapoor and Mr. Vijay Jadhao for help in computation.

The author is thankful to his friend, Dr. A. P. Pathak for his cooperation and for a pleasant and memorable association with him. Thanks are also due to many teachers and colleagues for their kind help and cooperation.

The author wishes to acknowledge his gratefulness to Principal K. D. Gadiya, P.G. Centre (Physics), J.E.S. College (Marathwada University), Jalna (Maharashtra) for his interest in this work and for the grant of study leave.

Financial assistance from the Council of Scientific and Industrial Research, New Delhi and Indian Institute of Technology, Kanpur is gratefully acknowledged. Finally, the author wishes to thank Mr. Nihal Ahmad for patiently and efficiently typing the manuscript, and M/s H. K. Panda and Lallu Singh for cyclostyling.

## TABLE OF CONTENTS

Chapter		Page
	LIST OF TABLES	v
	LIST OF FIGURES	vi
	SYNOPSIS	vii
I.	INTRODUCTION	1
II.	THE GREEN'S FUNCTION METHOD	4
	2.1 Green's Functions - Definition	4
	2.2 The Description of the Method	6
III.	ELASTIC SCATTERING OF ELECTRONS FROM SEMI-INFINITE CRYSTALS	13
	3.1 Introduction	13
	3.2 Variational Principle for Scattering Problems	16
	3.3 Elastic Scattering from One-Dimensional Potential Step	18
	3.4 Scattering from Three-Dimensional Semi-Infinite Crystals	20
	3.5 The Green's Function	22
	3.6 Structure Factors and Bethe Condition	24
	3.7 Muffin-Tin Potential and Evaluation of Intensity	25
	3.8 Discussion	29
IV.	LEED SPECTRUM AND BAND STRUCTURE OF ALUMINIUM	31
	4.1 Formulation	31
	4.2 Band Structure Calculations	34
	4.3 Results and Discussion	36
V.	ELECTRONIC STRUCTURES OF BERYLLIUM AND TITANIUM	40
	5.1 Introduction	40
	5.2 Brief Account of the Method	41
	5.3 Description of the Calculation	44
	5.4 Results and Discussion	51
VI.	CONCLUSION	64
	REFERENCES	67
	APPENDIX	70

**LIST OF TABLES**

<b>Table</b>		<b>Page</b>
I	Points of 1/24 of the Brillouin zone where energy eigenvalues are computed.	46
II	Bandwidths	53
III	Heat capacities	58
IV	Bandwidth and d bandwidth of Titanium	62

## LIST OF FIGURES

Figure		Page
1.	Energy band structure of Al along $\Delta$ -axis	35
2.	Comparison between measured and calculated beam intensities versus energy for the (0,0) beam from the (100) surface of Al, normal incidence	37
3.	Comparison between measured and calculated beam intensities versus energy for the (0,0) beam from the (100) surface of Al, normal incidence.	38
4.	The B.Z. for the hcp crystal with the 1/24 zone and crystal symmetry directions.	45
5.	The energy bands of Beryllium along symmetry directions.	50
6.	The energy bands of Titanium along symmetry directions.	52
7.	Density of states for Beryllium.	55
8.	Density of states for Titanium.	57
9.	Band structure of Titanium for different electronic configurations and different values of exchange parameter.	60

## SYNOPSIS

GREEN'S FUNCTION METHOD FOR ELECTRON DIFFRACTION  
AND BAND STRUCTURE PROBLEMS

Vibhakar Vasantrao Bhokare  
Ph.D.

Department of Physics  
Indian Institute of Technology, Kanpur  
December 1973

The Green's function method of electronic band structure calculation due to Korringa-Kohn-Rostoker is a powerful computational tool which has the virtue of rapid convergence of eigenvalues. But it has not found as much application as it deserves because a straightforward application of the method requires enormous computational efforts in many cases. Methods similar to the Green's function method have also been formulated in the past for the LEED [Low-Energy Electron-Diffraction] problem excluding surface effects. But there was no actual numerical computation with such methods due to the computational difficulties. The present thesis, "Green's Function Method for Electron Diffraction and Band Structure Problems", attempts to get actual numerical results both for the electron scattering problem and the band structure problem of hcp [hexagonal close-packed] lattices, after proper formulation and careful simplification of the Green's function method. The results show that in spite of the approximations involved in the variational procedure used, one gets reasonably good numerical estimates for the electron scattering problem. The results for electronic band structure of Beryllium and Titanium are close to those obtained by the APW [Augmented Plane Wave] method.

The problem of elastic scattering of electrons from semi-infinite perfect crystals is considered first. This problem arose from and is intimately connected with what is now the vast and complicated subject of LEED problem. An approximate variational approach is described for computing elastic scattering of electrons from the perfect semi-infinite crystals. It is shown that the Green's function method of electronic band structure calculation can be conveniently used for such computations with the assumption of muffin-tin potential at the lattice sites. Numerical computation of the intensity in the (0,0) direction for Aluminium crystal is carried out. In this connection, the high-energy band structure of Aluminium is also computed. Results for (0,0) intensity is compared with some theoretical and experimental results of LEED for Aluminium. The variation method described here immensely simplifies the calculation and yields fairly good results. It may therefore be used as a quick and inexpensive method for computing elastic LEED intensities.

The problem of computing electronic band structure of hcp metals by Green's function method is considered next. Although this method has been used extensively for the cubic metals, it has found very limited application to other structures, mainly due to the computational difficulties for complex lattices and inadequacy of muffin-tin approximation. However, the case of hcp metals is interesting because muffin-tin approximation in this case is comparable to that for face-centred cubic metals. Therefore, it appeared worth-while to study hcp metals by Green's function method and exploit its virtue of convergence of eigenvalues with small size determinants. The Kohn-Rostoker method for complex crystals is

employed and group-theoretical factorization of the secular determinant is performed by using the symmetry-adapted hexagonal harmonics, which greatly simplified the computation. Using this method the band structures of Beryllium and Titanium are computed. With enough experimental data on band structure, Beryllium is an interesting test case. Titanium is a typical transition metal and with little experimental data and limited theoretical calculations, it is expected to exhibit the general features of hcp metals. The energy-bands, Fermi energies, density-of-states curves, and coefficients of electronic specific-heat are computed for both, Beryllium and Titanium. The results are compared with the earlier theoretical and experimental results, and they are found to be in good agreement. The band structure of Titanium with respect to its exchange parameter,  $\lambda$ , is studied at preliminary level. Although sufficient experimental data on its band structure and Fermi surface are required to definitely fix the value of the exchange parameter, it is concluded that  $2/3 < \lambda < 3/4$  is the most interesting range.

The final conclusion of the study presented in the thesis is that with proper formulation and careful simplification, it is possible to employ the Green's function method of Korringa-Kohn-Rostoker both for the electron scattering problem and the problem of electronic structure of hcp metals leading to quite satisfactory numerical results.

## CHAPTER I

### INTRODUCTION

The Green's function method of electronic band structure calculation for perfect solids was first proposed by Korringa,<sup>1</sup> in 1947. His approach was based upon the multiple scattering of electron waves in solids [solid being considered as assembly of spherical scatterers]. Later, the same method was proposed on different lines by Kohn and Rostoker,<sup>2</sup> in 1954. A variational procedure was introduced by them to solve the integral form of the Schrödinger's equation for an electron in a periodic potential. Though these two procedures were independently given, they are essentially equivalent and are often called the KKR [Korringa-Kohn-Rostoker] method.

From a mathematical point of view, it has the virtue of rapid convergence of eigenvalues. This is intimately connected with the fact that the method deals with the scattering of slow electrons in a periodic potential, by employing the expansion of the Bloch waves in spherical harmonics. It has proved to be rapidly convergent owing to the well-known fact, that the partial wave analysis for scattering by single atoms is rapidly convergent for slow electrons.

Computation-wise the Green's function method is a powerful tool. But the method has not found as much application as it deserves, mainly because a straightforward application of the method requires considerable

computational efforts. In many cases, proper formulation and careful simplification is essential to extract numerical results. Such an attempt will be made in the present thesis, where numerical results are obtained for both the electron scattering problem and the band structure problem of hcp [hexagonal close-packed] structures.

The KKR method seems to be very useful for theoretical investigation of the low energy electron scattering from crystals because basically it is a scattering theory. In fact, in the recent years, the KKR type formalisms for LEED [Low-Energy Electron-Diffraction] intensity calculations have been given by many workers<sup>3-7</sup> including the author.<sup>8</sup> The fact that intimate connection exists between the electron-diffraction theory and the band theory, is very helpful for LEED intensity calculation in view of the detailed computational facilities existing for the band structure calculation. The study of elastic scattering of the low energy electrons from the perfect semi-infinite lattices constitutes the first part of this dissertation, where it will be shown that the well-known KKR method can be used conveniently for the computation of electron-diffraction intensities with the additional assumption of muffin-tin potential at the lattice sites.

Although the KKR method was formulated in 1954 it was put to widespread practical use in 1961 by Ham and Segall<sup>9</sup> who modified the KKR procedure in several important respects. After that in the last decade, the method has been extensively applied for the energy band calculation of the cubic metals.<sup>10</sup> But the method has found limited<sup>11</sup> application to structures other than the cubic metals, due to the

inadequacy of muffin-tin approximation and the computational difficulties for the complex crystals. However, the case of the hcp metals is interesting because muffin-tin approximation in this case is comparable to that for the fcc [face-centred cubic] metals. Therefore, it appears worth-while to apply the method to hcp metals and exploit its virtue of convergence of eigenvalues with small size secular determinants. The electronic band structure of hcp metals will be described in the later part of this work. The KKR formalism for complex crystals<sup>12</sup> [i.e., crystals with more than one atom per unit cell] will be employed and group-theoretical factorization<sup>13</sup> of the determinant will be described which immensely simplifies the computation.

## CHAPTER II

### THE GREEN'S FUNCTION METHOD

Since the comprehensive reviews of the Green's function method are available in the literature,<sup>2,9,10</sup> only a brief account of the method is presented in this chapter for the sake of completeness. In the following sections, we give definition of Green's functions followed by the description of the method.

#### 2.1 Green's Functions - Definition:

Consider the inhomogeneous equation

$$\hat{L} \psi(\underline{r}) - \lambda \psi(\underline{r}) = Q(\underline{r}), \quad (2.1)$$

with  $\hat{L}$  a Hermitian differential operator, with  $Q(\underline{r})$  a continuous function of the variable  $\underline{r}$ , and  $\lambda$  a given constant. The function  $\psi(\underline{r})$ , which satisfies (2.1), obeys the usual type of the homogeneous boundary conditions.

Formally, then, a particular "solution" of (2.1) is conveniently constructed in terms of the Green's function  $G(\underline{r}, \underline{r}')$  for the operator  $[\hat{L} - \lambda]$  and the given boundary conditions as:

$$\psi(\underline{r}) = \int_{\text{Over Entire Space}} G(\underline{r}, \underline{r}') Q(\underline{r}') d\underline{r}', \quad (2.2)$$

an integral equation for  $\psi(\underline{r})$ .

The Green's function,  $G(\underline{r}, \underline{r}')$ , is defined as that solution of (2.1) for which  $G(\underline{r}) = \delta(\underline{r}-\underline{r}')$ . Thus the Green's function satisfies the equation

$$\hat{L}G(\underline{r}, \underline{r}') - \lambda G(\underline{r}, \underline{r}') = \delta(\underline{r}-\underline{r}'), \quad (2.3)$$

with the same boundary conditions as on the function  $\psi(\underline{r})$ .

The Green's function is of much theoretical importance because it transforms a differential equation with suitable boundary conditions to an integral equation. And, the statement of a problem in integral form is preferred to that in differential form since the integral form is a complete statement of the problem in the sense that it contains the boundary conditions associated with the problem. Moreover, sometimes there is mathematical convenience and ease with integral equations.

Now, consider the three-dimensional one-electron Schrödinger equation in atomic units:

$$[\nabla^2 - U(\underline{r}) + E] \psi(\underline{r}) = 0, \quad (2.4)$$

where  $U(\underline{r})$  and  $E$  are potential energy and total energy, respectively. This is the basic equation to be solved for the electron diffraction and the band structure problems, with different boundary conditions, where  $U(\underline{r})$  is a potential energy of an electron in a tri-periodic crystal.

Treating,  $U(\underline{r}) \psi(\underline{r}) = V(\underline{r})$ , in (2.4) temporarily as a given inhomogeneity even though it contains the unknown function  $\psi(\underline{r})$ , it may be written as

$$[\nabla^2 + E] \psi(\underline{r}) = \mathbf{v}(\underline{r}). \quad (2.5)$$

On comparing (2.5) with (2.1), it becomes obvious that the Green's function for the differential operator  $[\nabla^2 + E]$  will satisfy

$$[\nabla^2 + E] G(\underline{r}, \underline{r}') = \delta(\underline{r} - \underline{r}'), \quad (2.6)$$

and the particular solution of (2.5) will be given by an integral equation like (2.2).

## 2.2 The Description of the Method :

For the band structure problem, one seeks solutions of the Schrödinger equation (2.4) for a potential  $U(\underline{r})$  which is periodic in lattice translations, so that the Bloch condition

$$\psi(\underline{r} + \underline{r}_s) = e^{i\mathbf{k} \cdot \underline{r}_s} \psi(\underline{r}) \quad (2.7)$$

is satisfied. Here  $\mathbf{k}$  is the crystal momentum vector, and  $\underline{r}_s$  is any translation vector of the crystal lattice. Equation (2.4) is in atomic units where unit of length is Bohr radius and unit of energy is Rydberg.

Generally, one is interested in calculating the energy values,  $E = E(\mathbf{k})$ , as a function of arbitrary  $\mathbf{k}$  lying within the first Brillouin zone [B.Z.] of the reciprocal lattice space for which solutions of the form of (2.7) exist.

Kohn-Rostoker<sup>2</sup> proceeded to solve this problem from the equivalent formulation that  $\psi(\underline{r})$  is also a solution to the integral equation (2.2), where  $G(\underline{r}, \underline{r}') = G(\underline{r} - \underline{r}')$  satisfies (2.6) and  $\mathcal{G}(\underline{r}) = \mathbf{v}(\underline{r})$ .

Since  $U(\underline{r})$  is a periodic potential,

$$U(\underline{r}) = \sum_s V(\underline{r} - \underline{r}_s),$$

where  $V(\underline{r} - \underline{r}_s)$  is the potential at  $\underline{r}$  due to the ion at the  $s^{\text{th}}$  lattice site,  $\underline{r}_s$ . For "muffin-tin" [m.t.] model of potential  $V(\underline{r})$ , that is, if  $V(\underline{r})$  is spherically symmetric within a sphere of radius  $r_i$  centred around each ion and inscribed in the unit cell [Here a "simple" crystal is considered with a single ion in each unit cell and a centre of inversion at the ion], and if  $V(\underline{r})$  is constant in the region between the spheres with which the zero of the energy is made to coincide; then the integral equation

$$\begin{aligned}\Psi(\underline{r}) &= \int G(\underline{r}, \underline{r}') U(\underline{r}') \Psi(\underline{r}') d\underline{r}' \\ &= \sum_{s'} \int G(\underline{r}, \underline{r}') V(\underline{r}' - \underline{r}_s) \Psi(\underline{r}') d\underline{r}'\end{aligned}$$

is a sum of contribution from the separate cells. Since the muffin-tin spheres do not overlap, this is really speaking a sum of the separate integrals, as may be demonstrated by introducing a variable  $\underline{p}$  such that  $\underline{r} = \underline{r}_s + \underline{p}$  in the cell around the lattice site  $\underline{r}_s$ . Thus

$$\Psi(\underline{r}_s + \underline{p}) = \sum_{s'} \int_{\substack{\text{over cell} \\ \text{vol. } \mathcal{V}}} G(\underline{r}_s + \underline{p}, \underline{r}_{s'} + \underline{p}') V(\underline{p}') \Psi(\underline{r}_{s'} + \underline{p}') d\underline{p}'.$$

Using Bloch condition (2.7),

$$\begin{aligned}\Psi(\underline{p}) &= \int \left[ \sum_s e^{i \underline{k} \cdot (\underline{r}_s - \underline{r}_s)} G(\underline{p} - \underline{p}' + \underline{r}_s - \underline{r}_s) \right] V(\underline{p}') \Psi(\underline{p}') d\underline{p}' \\ &= \int G(\underline{p}, \underline{p}') V(\underline{p}') \Psi(\underline{p}') d\underline{p}',\end{aligned}\quad (2.8)$$

where,  $\mathcal{G}(\underline{\ell}, \underline{\ell}') = \sum_{\underline{s}''} e^{i\underline{k} \cdot \underline{r}_{\underline{s}''}} G(\underline{\ell}, \underline{\ell}' + \underline{r}_{\underline{s}''})$ , is known as the "Structural Green's Function", and  $\underline{r}_{\underline{s}''} = \underline{r}_{\underline{s}}, -\underline{r}_{\underline{s}}$ . Henceforth, the variables  $\underline{\ell}$  and  $\underline{\ell}'$  will be denoted by  $\underline{r}$  and  $\underline{r}'$ , respectively.  $\mathcal{G}(\underline{r}, \underline{r}')$  is a function of two variables  $\underline{r}$  and  $\underline{r}'$  which refer to the points in the same unit cell.

The integral equation (2.8) has interesting implication that in order to solve the band structure problem, it is sufficient to consider the solutions of the Schrödinger equation

$$[\nabla^2 - V(\underline{r}) + E] \Psi(\underline{r}) = 0,$$

within a single unit cell only.

The Green's function,  $\mathcal{G}(\underline{r}, \underline{r}')$ , may also be written as

$$\mathcal{G}(\underline{r}, \underline{r}') = -\frac{1}{V} \sum_n \frac{e^{i(\underline{k} + \underline{K}_n) \cdot (\underline{r} - \underline{r}')}}{[(\underline{k} + \underline{K}_n)^2 - E]} , \quad (2.9)$$

where  $V$  is the unit cell volume and the sum runs over all reciprocal lattice vectors  $\underline{K}_n$ . It is evident from (2.9) that  $\mathcal{G}(\underline{r}, \underline{r}')$  is a function of  $\underline{k}$  and  $E$ , and satisfies the relations:

$$\mathcal{G}(\underline{r}', \underline{r}) = \mathcal{G}^*(\underline{r}, \underline{r}'), \quad (2.10)$$

and

$$\mathcal{G}(\underline{r} + \underline{r}_s, \underline{r}') = e^{i\underline{k} \cdot \underline{r}_s} \mathcal{G}(\underline{r}, \underline{r}').$$

Kohn-Rostoker<sup>2</sup> introduced a variational procedure leading to a stationary value for the energy to solve the integral equation (2.8). The integral equation (2.8) may be derived from the variation principle

$$\delta \Delta = 0,$$

where

(2.11)

$$\Delta \equiv \int_{\mathcal{V}} \psi^*(\underline{r}) v(\underline{r}) \psi(\underline{r}) d\underline{r} - \int_{\mathcal{V}} \int_{\mathcal{V}} \psi^*(\underline{r}) v(\underline{r}) G(\underline{r}, \underline{r}') v(\underline{r}') \psi(\underline{r}') d\underline{r}' d\underline{r}$$

This variational principle has the important property that  $\delta \Delta$  vanishes in first order for all variations from the solution of (2.8) regardless of whether or not the variations satisfy the boundary conditions.

For proper handling of the singularities of  $G$ , a limiting procedure such as

$$\Delta = \lim_{\epsilon \rightarrow 0} \Delta_\epsilon,$$

where

(2.12)

$$\Delta_\epsilon = \int_{r < r_i - 2\epsilon} dr \psi^*(\underline{r}) v(\underline{r}) [\psi(\underline{r}) - \int_{r' < r_i - \epsilon} G(\underline{r}, \underline{r}') v(\underline{r}') \psi(\underline{r}') d\underline{r}'],$$

is used.  $\epsilon$  is a positive quantity, and  $r_i$  is the muffin-tin radius. For an arbitrary potential, even this variational procedure would be extremely complicated to use. However, the method simplifies enormously for the muffin-tin potentials [Muffin-tin approximation is precisely the major limitation of the method]. If the zero of energy is made to coincide with the constant value of the potential in the region outside the spheres, then the integrals in (2.8) and (2.12) receive a nonzero contribution only from the part of the unit cell within the sphere. A trial function of the form,

$$\psi(\underline{r}) = \sum_{l=0}^{l_{\max.}} \sum_j i^l c_{lj} R_l(r) Y_{lj}(\theta, \phi), \quad (2.13)$$

is used within the inscribed sphere.  $R_l(r)$  is a radial function which is finite at  $r=0$  and satisfies the radial differential equation

$$\left[ -\frac{1}{r^2} \frac{d}{dr} \left( r^2 \frac{d}{dr} \right) + \frac{1(l+1)}{r^2} + V(r) - E \right] R_1(r) = 0 \quad (2.14)$$

The functions  $\Lambda_{1j}(\theta, \phi)$  are the lattice harmonics<sup>9</sup> which are linear combinations of spherical harmonics of angular momentum 1. They are normalized, real, and mutually orthogonal. Finally,  $C_{1j}$  are coefficients to be treated variationally.

Then, Kohn-Rostoker have shown that the variational principle leads to a set of linear homogeneous equations

$$\sum_{l'=0}^{l_{\max}} \sum_{j'} \Lambda_{1j, l' j'} C_{l' j'} = 0. \quad (2.15)$$

$\Lambda_{1j, l' j'}$  will be given explicitly below. The condition that the set of equations (2.15) have a nontrivial solution is the one that determines the value of  $E$  appropriate to the given  $k$  [or value of  $k$  along, say, a line, for given  $E$ ], namely

$$\det \left| \Lambda_{1j, l' j'} \right| = 0. \quad (2.16)$$

If in the expansion (2.13) of the trial function,  $l_{\max}$  is taken sufficiently large, the root of (2.16) approaches arbitrarily close to the desired eigenvalue  $E = E(k)$  of (2.4). In practice, this convergence is extremely good, and it usually suffices to have  $l_{\max} = 2$ .

The expansion of  $G(r, r')$  for  $E > 0$  and  $r < r' < r_i$  is given by

$$\begin{aligned} G(r, r') = \sum_{1,j} \sum_{1',j'} \left[ i^{(1-1')} B_{1j, 1'j'} j_1(kr) j_{1'}(kr') + k \delta_{11'} \delta_{jj'} j_1(kr) j_{1'}(kr') \right] \\ \times \Lambda_{1j}(\theta, \phi) \Lambda_{1'j'}(\theta', \phi'), \end{aligned} \quad (2.17)$$

where  $\kappa = \sqrt{E}$ ,  $j_1$  spherical Bessel function, and  $\eta_1$  Neumann function.

$\Lambda_{1j,1'j'}$  are then given in terms of  $B_{1j,1'j'}$  as:

$$\Lambda_{1j,1'j'} = R_1(r_i)R_{1'}(r_i)Q_1(j_1)Q_{1'}(j_{1'})\lambda_{1j,1'j'}, \quad (2.18)$$

where we define

$$Q_1(j_1) = j_1(\kappa r_i) \cdot \left[ \frac{1}{R_1(r)} \frac{dR_1(r)}{dr} - \frac{1}{j_1(\kappa r)} \frac{dj_1(\kappa r)}{dr} \right]_{r=r_i}. \quad (2.19)$$

Similar definition holds for  $Q_1(\eta_1)$ , and

$$\lambda_{1j,1'j'} = \left[ B_{1j,1'j'} + \kappa \delta_{11'} \delta_{jj'} \frac{Q_1(\eta_1)}{Q_1(j_1)} \right], \quad (2.20)$$

where  $B_{1j,1'j'}$  are "Structure Constants".

The above expressions are appropriate for  $E > 0$ , this zero of the energy scale is with respect to the constant value of the muffin-tin potential. The expressions for the case of  $E < 0$  are given in Ref. 9. The same reference also contains the details about the structure constants.

One great advantage of the Green's function method is that the structure part and the atomic part appear separately in the elements of the secular determinant. Apart from a scaling factor, the structure constants, constituting the structure part of the elements, are independent of the lattice constants. Therefore, although the structure constants are fairly complicated functions, they may be computed once and for all for a given crystal structure. At the symmetry points for which the expansion (2.13) for  $l_{\max.} = 2$  admits only two or three independent terms, the actual evaluation of the  $(2 \times 2)$  or  $(3 \times 3)$  determinant of the  $\Lambda_{1j,1'j'}$  and the determination of the root of the secular equation (2.16)

may in fact be carried out with the use of a desk calculator, once structure constants are available. Alternatively, with availability of high speed digital computer, one can of course compute the required structure constants directly as a part of each run.

In the application of the Green's function method, therefore, one has to evaluate the structure constants for a sequence of values of  $E$  for given  $k$ , or for a sequence of values of  $k$  for given  $E$ . Next, the spherical Bessel functions and Neumann functions and their derivatives are obtained. The logarithmic derivatives,  $L_1 = \left[ \frac{1}{R_1(r)} \frac{dR_1(r)}{dr} \right]_{r=r_i}$ , are obtained by numerical integration of the radial equation. The determinant of  $\Delta_{1j,1'j'}$  is then calculated, and the root of the secular equation (2.16) is found either graphically or by interpolation schemes.

## CHAPTER III

### ELASTIC SCATTERING OF ELECTRONS FROM SEMI-INFINITE CRYSTALS

#### 3.1 Introduction:

A fundamental problem of the theory of electron-diffraction is elastic scattering of electrons from the semi-infinite perfect crystals. This problem of elastic scattering from the semi-infinite crystals arose from and is very closely related to what is at present the vast and complicated subject of LEED [Low-Energy Electron-Diffraction] problem.

In 1928, a theory for LEED phenomenon was first proposed by Bethe.<sup>14</sup> His historical approach was an idealization of LEED problem as elastic scattering of the incident electrons from the periodic crystal potential. Then in principle it was a matter of matching the wave functions and their derivatives at the crystal surface. But this in actual practice involves lengthy computation before any reasonable result can be extracted out of it because of the slow convergence of the plane wave expansion for Bloch waves. The convergence difficulty was circumvented by Boudreux and Heine<sup>15</sup> who suggested the use of a pseudopotential instead of the crystal potential in Bethe's matching formalism. They also pointed out the need to add evanescent waves to the superposition of Bloch waves used by Bethe. Similar type of formulation was also developed by Marcus and Jepsen.<sup>16</sup> All these techniques have certain

inherent difficulties like detailed calculation of the wave field inside the crystal and proper matching of the wave functions and their derivatives at the boundary. Various other approaches<sup>3-7,17-24</sup> were proposed incorporating more realities for the LEED problem like surfaces etc. and using different approximations. But there also required heavy computation and the computational difficulty continued. Recently, some elaborate and extensive computations<sup>7,23-26</sup> were carried out on LEED, where the important inelastic effects for LEED were accounted for, and led to very good agreement with experiments. Still the basic computational aspect of the earliest and simplest idealization of LEED, as elastic scattering of electrons from the semi-infinite periodic lattices, remained unchanged.

The reasons, why one should pay attention towards the computational aspect and the detailed understanding of elastic scattering from the semi-infinite perfect crystals, are as follows: (i) Presently, the exact force law between an electron and a crystal is mostly unknown, and there is need to study elastic scattering in order to understand which of the predictions from such considerations of elastic scattering are sensitive to the various aspects of a force law describing the electron-crystal interaction.

Calculations in this spirit have been done before.<sup>25,26</sup> (ii) Experimentalists usually find it difficult to get into heavy computations to explain the observed intensities. They would prefer computationally simple and quick methods giving fairly good results to the complicated ones producing very accurate results. (iii) Understanding of elastic scattering in details is very helpful to have a clear-cut distinction of elastic effects and those due to inelastic scattering and surface effects.

Here the Green's function method of energy band theory is properly formulated to be applicable in electron-diffraction theory. The KKR type formalisms for LEED problem are already there in the literature.<sup>3-7</sup> But we describe an approximate variational treatment<sup>8</sup> of the problem which leads to satisfactory results without involving much computation subject to the availability of standard programmes for band structure calculation by KKR method. We consider the model like Kerre and Phariseau<sup>5</sup> and others which assumes muffin-tin potential at the lattice sites of the semi-infinite crystal and treats the problem variationally. General variational procedure for one-dimensional case is given by Shen and Krieger,<sup>27</sup> and Shen<sup>6</sup> has also considered the case of the three-dimensional semi-infinite crystal. The virtue of the variational approach is that neither exact boundary between the crystal and the vacuum nor the detailed numerical value of the wave field inside the crystal are needed for the intensity calculation. All that is needed is a suitable trial wave function and the actual amount of computation involved depends on the size of the determinants<sup>27</sup> that one has to evaluate. However, there is no special computational advantage in a layer-by-layer variational calculation<sup>6</sup> over the more usual ones by other methods. Moreover, the Green's function of such approach leads to fairly cumbersome structure constants.

The above-mentioned difficulties of the variational approach are bypassed here by choosing Bloch wave as trial function. The wave vector of the Bloch wave is also treated variationally so that the approximation is more than a mere single Bloch wave approximation. Actually this amounts

to picking up the largest contributing Bloch wave from a combination such that its wave vector serves as a variational parameter. The choice of such an approximate trial function also finds sufficient justification in the final results obtained from it. It is shown that such trial function leads to the usual structural Green's function of KKR method and then using lattice harmonics<sup>9</sup> it is possible to show that the intensity is a ratio of two very small size determinants whose elements can be formed out of those of the KKR secular determinant. Though the KKR type formalism is not new for this problem it never yielded to computation as simply and as quickly as the present one. However, the present approach will have the limitations of being applied only to the case of elastic scattering [E-LEED<sup>26</sup>] intensities because of the constraint of using a static real potential.

### 3.2 Variational Principle for Scattering Problems:

The variational methods are very useful especially when perturbation methods become tedious and complex to use. Usually a single physical entity, in which one is interested, is given by a variational principle that leads to a stationary expression. Because of the stationary characteristic of the variational equation and its consequent insensitivity towards the errors in the trial function, it is often possible to obtain very good estimates for the physical entity under consideration with a relatively crude trial function. Obviously, this is a property of great significance in practical calculations.

Variational principle has been quite successful for the binding energy in atomic physics, scattering phase shifts in nuclear physics, and band theory in solid state physics. It is also well known that the variational method can, in general, be applied fruitfully to the potential scattering problems. We describe, in this chapter, the use of variational principle for elastic scattering from (a) one-dimensional potential step, and (b) three-dimensional semi-infinite perfect crystal. In the following, we state the variational principle for reflection amplitude for one- and three-dimensional scattering problems.

Consider the case of elastic scattering in one-dimension from a potential  $V(x)$  that is non-vanishing for  $0 \leq x \leq \infty$ . The corresponding variational principle for the reflection coefficient  $R$  is

$$\delta R = 0, \quad (3.1)$$

and  $R$  is given by<sup>27</sup>

$$R = \left( -\frac{i}{2k_0} \right) \left[ \frac{\left[ \int e^{ik_0 x} V(x) \psi(x) dx \right]^2}{\int dx \psi(x) V(x) [\psi(x) - \int G(x, x') V(x') \psi(x') dx']} \right], \quad (3.2)$$

where  $\psi(x)$  is the trial wave function,  $k_0$  is the wave number of the incident plane wave,  $\exp(ik_0 x)$ ;  $k_0^2 = E$ , the total energy, and the Green's function  $G$  is given by:  $G(x, x') = -(i/2k_0) \exp(ik_0 |x-x'|)$ .

For three-dimensional scattering problem, the variational principle for the reflection amplitude  $T$  which is a function of scattered wave vector  $\underline{k}_s$  and incident wave vector  $\underline{k}_i$  is

$$\delta T = 0, \quad (3.3)$$

where<sup>28</sup>

$$T(k_s, k_i) = \left[ \frac{\left[ \int \psi^*(\underline{r}) U(\underline{r}) e^{ik_i \cdot \underline{r}} d\underline{r} \right] \left[ \int e^{-ik_s \cdot \underline{r}} U(\underline{r}) \psi(\underline{r}) d\underline{r} \right]}{\int \psi^*(\underline{r}) U(\underline{r}) \left[ \psi(\underline{r}) - \int G(\underline{r}, \underline{r}') U(\underline{r}') \psi(\underline{r}') d\underline{r}' \right] d\underline{r}} \right]. \quad (3.4)$$

The  $\delta T$  vanishes for arbitrary variations of  $\psi$ . Here  $G(\underline{r}, \underline{r}')$  is the Green's function satisfying (2.6),  $U(\underline{r})$  is the potential in atomic units, and  $\psi(\underline{r})$  is the trial wave function.

### 3.3 Elastic Scattering From One-Dimensional Potential Step:

We consider here, as an illustration, the problem of elastic scattering of electrons from one-dimensional potential step using variational procedure. In expression (3.2), it is possible to expand  $\psi(x)$  in terms of a complete set of functions  $\phi_i(x)$  as<sup>27</sup>

$$\psi(x) = \sum_{i=1}^n c_i \phi_i(x), \quad (3.5)$$

and choose  $c_i$  variationally to get the condition determining R:

$$\det \begin{vmatrix} F_{ij} + \frac{i}{2k_o R} D_i D_j \end{vmatrix} = 0, \quad (3.6)$$

where

$$F_{ij} \equiv \int \phi_i(x) V(x) \left[ \phi_j(x) - \int G(x, x') V(x') \phi_j(x') dx' \right] dx, \quad (3.7)$$

and

$$D_i \equiv \int \phi_i(x) V(x) e^{ik_o x} dx.$$

For one-dimensional potential step

$$V(x) = \begin{cases} 0, & x < 0 \\ V_0, & x > 0 \end{cases}, \quad (3.8)$$

where  $V_0$  is some constant value, and our choice of trial wave function

$$\psi(x) = C(k) e^{ikx}, \quad (3.9)$$

with  $k$  in general complex; we have

$$\begin{aligned} D_1 &= \left[ \frac{iV_0}{(k + k_0)} \right], \\ F_{11} &= \left[ \frac{iV_0 (kk_0 + k_0^2 - V_0)}{2kk_0(k+k_0)} \right], \end{aligned} \quad (3.10)$$

and

$$R = \left[ \frac{V_0 k}{[k_0^3 + 2kk_0^2 + (k^2 - V_0)k_0 - V_0 k]} \right].$$

If we want  $R$  to be extremum with respect to the variational parameter  $k$ , this extremum condition leads to:

$$E = E(k) = (k^2 + V_0) \quad (3.11)$$

This is nothing but the energy wave vector relation for the case of one-dimensional potential step.

For  $E < V_0$ ,  $k = ik$ , where  $k = (V_0 - E)^{\frac{1}{2}}$ , which leads to the wave function  $e^{-kx}$ , and the reflected intensity is

$$|R|^2 = 1. \quad (3.12)$$

For  $E > V_0$ ,  $k = (E - V_0)^{\frac{1}{2}}$ , which is real, leads to the wave function  $e^{ikx}$ , and reflected intensity is

$$|R|^2 = \left[ \frac{1 - \mu}{1 + \mu} \right]^2, \quad (3.13)$$

where,  $\mu = k/k_0$ , is called the index of refraction. Results (3.12) and (3.13) obtained here without using the usual matching procedure are the same as obtained by the procedure of matching at the boundary.

The important conclusion from this consideration is that the extremum condition for  $R$  leads to proper energy wave vector relation. For periodic potential the extremum condition would mean the energy band structure relation.<sup>27</sup> Actually, this is intimately related to the fact that energy band structure essentially governs the diffraction. Conversely, one can obtain the usual results variationally by choosing a wave function like (3.9) with  $k$  satisfying the known energy wave vector relationship. Thus  $R$  as a function of  $k$  is extremum for those values of  $k$  that satisfy the band structure relationship for the given energy when the potential is periodic.

### 3.4 Scattering From Three-Dimensional Semi-Infinite Crystals:

The simple model of a semi-infinite perfect crystal is as follows. The lattice extends from  $-\infty$  to  $+\infty$  in  $x$  and  $y$  directions, and from 0 to  $+\infty$  in  $z$  direction. It is assumed that the crystal is a "simple crystal" having one atom per unit cell. Only elastic scattering is considered here.

The reflected intensity in case of three-dimensional scattering is

$$I = |T|^2 / 16\pi^2 , \quad (3.14)$$

where  $T$  is given by the relation (3.4).

For elastic scattering

$$|\underline{k}_i| = |\underline{k}_s| = k, \quad (3.15)$$

and here

$$k^2 = E.$$

$E$  is the energy of the incident electrons. For diffraction from the perfect three-dimensional crystals, the potential is given by

$$U(\underline{r}) = \sum_s V(\underline{r} - \underline{r}_s), \quad (3.16)$$

where  $V(\underline{r} - \underline{r}_s)$  is the potential at  $\underline{r}$  due to the ion at the lattice site  $\underline{r}_s$ . In case of the semi-infinite crystal,  $\underline{r}_s$  lies in the half space of  $z \geq 0$ . Then  $U(\underline{r})$  given by (3.16) is not periodic in translations along  $z$ -axis.

Now, it is a matter of choosing an appropriate trial function  $\psi(\underline{r})$ . Note that it must have Bloch form along  $x$  and  $y$  axis due to periodicity in those directions.

We assume the wave function  $\psi(\underline{r})$  within the crystal to have the following property

$$\psi(\underline{r}) = \psi_p(\underline{r}) = e^{-ip \cdot \underline{r}_s} \psi_p(\underline{r} + \underline{r}_s) \quad (3.17)$$

for  $\underline{r}$  and  $\underline{r}_s$  in the region  $z \geq 0$ . The crystal momentum is denoted by  $p$ . Thus, we are choosing a trial function which is exact for the  $x$  and  $y$  directions and which essentially contains the variational parameter  $p_z$  [z-component of  $p$ ]. This would lead to the evaluation of the intensity as a function of  $p_z$  which has to be extremized to get the actual intensity.

Then

$$T(\underline{k}_s, \underline{k}_i) = \left[ \frac{1}{\sqrt{N}} \sum_s e^{i(\underline{k}_i - \underline{p}) \cdot \underline{r}_s} \right] \times \left[ \frac{1}{\sqrt{N}} \sum_{s'} e^{i(\underline{p} - \underline{k}_s) \cdot \underline{r}_{s'}} \right] \times \Gamma(\underline{k}_s, \underline{k}_i), \quad (3.18)$$

where

$$\Gamma_{(k_s, k_i)} = \frac{\left[ \int \psi_p^*(\underline{r}) V(\underline{r}) e^{ik_i \cdot \underline{r}} d\underline{r} \right] \left[ \int e^{-ik_s \cdot \underline{r}} V(\underline{r}) \psi_p(\underline{r}) d\underline{r} \right]}{\int \psi_p^*(\underline{r}) V(\underline{r}) \left[ \psi_p(\underline{r}) - \frac{1}{N} \int \sum_{s,s'} G(\underline{r}, \underline{r}_s, \underline{r}' + \underline{r}_s) e^{ip \cdot (\underline{r}_s - \underline{r}_s')} V(\underline{r}') \times \psi_p(\underline{r}') d\underline{r}' \right] d\underline{r}} \quad \dots (3.19)$$

Here integration is over one unit cell and N is the total number of atoms in the crystal. Thus, one can evaluate T as a function of  $p_z$  and it is seen from the consideration of the one-dimensional problem that  $\frac{\partial T}{\partial p_z} = 0$  would give the  $p_z$  corresponding to energy E which may be used in  $T(p_z)$  to evaluate the intensity.

Thus, our evaluation of the intensity has all the virtues of the variational method. However, instead of taking a linear combination of Bloch waves, we have employed a single Bloch wave, the z-component of whose wave vector is treated as a variational parameter. This is essentially the limitation of our calculation. But it is comparable to the limitations of the treatment of LEED by dynamical theory with a single-Bloch-wave approximation,<sup>29</sup> or the usual two or three beam band matching calculations, the s-wave multiple scattering theories, and the second order perturbation calculation. At the same time, the simplicity and computational ease with our final expression is remarkable for numerical work. Much of the simplicity of the computation will be lost if a linear combination<sup>6</sup> of Bloch waves is chosen as the trial wave function.

### 3.5 The Green's Function:

Let us consider the Green's function in equation (3.19):

$$\begin{aligned}
 & \frac{1}{N} \sum_{s,s'} G(\underline{r} + \underline{r}_s - \underline{r}' - \underline{r}_{s'}) e^{i\underline{p} \cdot (\underline{r}_{s'} - \underline{r}_s)} \\
 &= \frac{1}{N} \sum_{s,s''} G(\underline{r} - \underline{r}' - \underline{r}_{s''}) e^{i\underline{p} \cdot \underline{r}_{s''}} \\
 &= \sum_{s''} G(\underline{r}, \underline{r}' + \underline{r}_{s''}) e^{i\underline{p} \cdot \underline{r}_{s''}} \\
 &= \mathcal{G}(\underline{r}, \underline{r}'),
 \end{aligned}$$

where  $\underline{r}_{s''} = \underline{r}_{s'} - \underline{r}_s$ .

Reduction of the double sum to obtain the result in the third step involves the use of the actual form for  $G(\underline{r}_s, \underline{r}_{s'})$  and the approximation that the terms of the order of  $1/N$  can be neglected. This can be seen by considering the one-dimensional case for simplicity [See Appendix].

It is easy to see that  $\underline{r}_{s''}$  is no longer confined to the half space  $z > 0$ . In fact, it is over the entire space and therefore is the usual KKR Green's function.<sup>2</sup> Hence, the expression for  $\Gamma(\underline{k}_s, \underline{k}_i)$  becomes:

$$\Gamma(\underline{k}_s, \underline{k}_i) = \frac{\left[ \int \Psi_p^*(\underline{r}) V(\underline{r}) e^{i \underline{k}_i \cdot \underline{r}} d\underline{r} \right] \left[ \int e^{-i \underline{k}_s \cdot \underline{r}} V(\underline{r}) \Psi_p(\underline{r}) d\underline{r} \right]}{\int \Psi_p^*(\underline{r}) V(\underline{r}) \left[ \Psi_p(\underline{r}) - \int \mathcal{G}(\underline{r}, \underline{r}') V(\underline{r}') \Psi_p(\underline{r}') d\underline{r}' \right] d\underline{r}}, \quad (3.20)$$

with  $\mathcal{G}(\underline{r}, \underline{r}')$  representing the usual KKR structural Green's function used in band structure calculation. This is not surprising because there exists an intimate relationship between the elastic scattering formalism and the KKR method of band theory. In fact, the work of Watts<sup>4</sup> establishes this connection and its use in the LEED theory. Here the variational version of this kind of approach is considered.

### 3.6 Structure Factors and Bethe Condition:

- It is very clear from the structure of relation (3.18) that the scattering intensity is proportional to

$$\frac{1}{N} \left| \sum_s e^{i(\underline{k}_i - \underline{p}) \cdot \underline{r}_s} \right|^2 \times \frac{1}{N} \left| \sum_{s'} e^{i(\underline{p} - \underline{k}_{s'}) \cdot \underline{r}_{s'}} \right|^2,$$

which equals

$$\frac{1}{N^{2/3}} \left| \sum_{\substack{s \\ r_{s_z}=0}} e^{i(k_{iz} - p_z) r_{sz}} \right|^2 \times \left| \sum_{\substack{s' \\ r_{s'_z}=0}} e^{i(p_z - k_{s'_z}) r_{s'z}} \right|^2, \quad (3.21)$$

when

$$\underline{k}_{i\parallel} = \underline{k}_{s\parallel} + \underline{g}\parallel, \quad (3.22)$$

and zero otherwise.

Here the symbols " $\parallel$ " and "z", in the subscripts of the vectors  $\underline{k}_i$ ,  $\underline{k}_s$  and  $\underline{g}$  [a reciprocal lattice vector], denote the parallel and perpendicular [i.e., z-component] components respectively to the crystal surface... of these vectors. This is because the summation over x and y components of  $\underline{r}_s$  and  $\underline{r}_{s'}$ , yield delta functions which vanish unless the condition (3.22) is satisfied. The condition (3.22) is nothing but the usual "Bethe Condition" that has emerged as it should from the structure factor parts of the variational calculation. This is comparable to the work of Watts<sup>4</sup> and Beeby<sup>21</sup> and arises from the two dimensional periodicity of the lattice parallel to the surface.

The two factors of (3.21) depend upon the particular crystal structure, and for cubic crystals one gets the following results:

(i) SC:

$$r_{s_z} = 1a, \quad \left| \sum_{l=0}^{\infty} e^{i(k_{i_z} - p_z)al/2} \right|^2 = \left[ \frac{1}{4 \sin^2 \frac{1}{2}(k_{i_z} - p_z)a} \right],$$

(ii) BCC:

$$r_{s_z} = \frac{1}{2}la, \quad \left| \sum_{l=0}^{\infty} e^{i(k_{i_z} - p_z)\frac{al}{2}} \right|^2 = \left[ \frac{1}{4 \sin^2 \frac{1}{4}(k_{i_z} - p_z)a} \right], \quad (3.23)$$

(iii) FCC:

$$r_{s_z} = \frac{1}{2}(1+m)a, \quad \left| \sum_{l=0}^{\infty} e^{i(k_{i_z} - p_z)r_{s_z}} \right|^2 = \left[ \frac{1}{16 \sin^4 \frac{1}{4}(k_{i_z} - p_z)a} \right],$$

where  $l$  and  $m$  are zero or positive integers, and "a" is the lattice constant.

### 3.7 Muffin-Tin Potential and Evaluation of Intensity:

We restrict our discussion to a potential,  $V(\underline{r})$ , of the muffin-tin form. It is then possible to expand the trial function as

$$\Psi_p(\underline{r}) = \sum_{l=0}^{1_{\max}} \sum_j i^l c_{lj}(p) R_l(r) Y_{lj}(\theta, \phi) \quad (3.24)$$

within the inscribed sphere.

We also expand,

$$e^{ik_i \cdot \underline{r}} = 4\pi \sum_{l,j} i^l j_l(kr) Y_{lj}(\theta, \phi) Y_{lj}(\theta_i, \phi_i), \quad (3.25)$$

where  $(\theta_i, \phi_i)$  and  $(\theta, \phi)$  are polar angles of  $\underline{k}_i$  and  $\underline{r}$ , respectively.

Now

$$\int \Psi_p^*(\underline{r}) V(\underline{r}) e^{i \underline{k}_i \cdot \underline{r}} d\underline{r} = \iint_{\text{surface}} \left[ e^{i \underline{k}_i \cdot \underline{r}} \frac{\partial \Psi_p^*(\underline{r})}{\partial \underline{r}} - \Psi_p^*(\underline{r}) \frac{\partial e^{i \underline{k}_i \cdot \underline{r}}}{\partial \underline{r}} \right] dS \quad (3.26)$$

Here use is made of the Green Theorem in vector analysis.

We define  $D_{1j}(\underline{k}_i)$  by

$$D_{1j}(\underline{k}_i) = 4\pi R_1(r_i) Q_1(j_1) \delta_{1j}(\theta_i, \phi_i), \quad (3.27)$$

and similar definition holds for  $D_{1j}(\underline{k}_s)$ .

Thus

$$\int \Psi_p^*(\underline{r}) V(\underline{r}) e^{i \underline{k}_i \cdot \underline{r}} d\underline{r} = \sum_{1,j} D_{1j}(\underline{k}_i) C_{1j}^*(p) \quad (3.28)$$

Similarly

$$\int \Psi_p(\underline{r}) V(\underline{r}) e^{-i \underline{k}_s \cdot \underline{r}} d\underline{r} = \sum_{1',j'} D_{1'j'}(\underline{k}_s) C_{1'j'}(p) \quad (3.29)$$

Thus the numerator of the relation (3.20) can be written as

$$\sum_{1,j;1',j'} D_{1j}(\underline{k}_i) D_{1'j'}(\underline{k}_s) C_{1j}^*(p) C_{1'j'}(p) \quad (3.30)$$

Similarly the denominator of (3.20) can be shown to be

$$\begin{aligned} & \int_{\substack{\text{vol. of} \\ \text{m.t.sph.}}} d\underline{r} \Psi_p^*(\underline{r}) V(\underline{r}) \left[ \int_{\substack{\text{surf. of} \\ \text{m.t.sph.}}} \Psi_p(\underline{r}') \frac{\partial \Phi(\underline{r}, \underline{r}')}{\partial \underline{r}'} - \Phi(\underline{r}, \underline{r}') \frac{\partial \Psi_p(\underline{r}')}{\partial \underline{r}'} \right] dS' \\ & \quad \text{at } \underline{r}' = \underline{r}_i \\ & = \sum_{1,j;1',j'} F_{1,j;1',j'} C_{1j}^*(p) C_{1'j'}(p). \end{aligned} \quad (3.31)$$

If the zero of energy is adjusted to coincide with the constant value of  $V(\underline{r})$  in the region outside the inscribed spheres, the integrals

in (3.31) differ from zero only within the inscribed spheres. Within the inscribed spheres  $V(\underline{r}) = V(r)$ , i.e., a spherically symmetric potential. The integrals are over the volume and surface of the muffin-tin spheres. It has been already shown that  $G(\underline{r}, \underline{r}')$  is the usual KKR structural Green's function. Therefore, the quantities  $F_{1j, 1'j'}$  are identical with  $\Delta_{1j, 1'j'}$  [See (2.18)]. Thus, denoting the combination  $(l, j)$  by  $n$

$$\Gamma_{(k_s, k_i, p)} = \left[ \frac{\sum_{n,n'} D_n(k_i) D_{n'}(k_s) C_n^*(p) C_{n'}(p)}{\sum_{n,n'} F_{n,n'} C_n^*(p) C_{n'}(p)} \right] \quad (3.32)$$

Now, Kohn<sup>30</sup> type transformations may be used to determine  $\Gamma_{(k_s, k_i, p)}$ .

Thus, for the case  $D_n(k_i) \neq D_n(k_s)$  we define  $f_n(p)$  by:

$$\begin{aligned} f_n(p) &= C_n(p), \quad n \geq 3 \\ f_1(p) &= \sum_n D_n(k_i) C_n(p) \end{aligned} \quad (3.33)$$

and

$$f_2(p) = \sum_n D_n(k_s) C_n(p)$$

to get

$$\sum_{n,m} F_{n,m} C_n^*(p) C_m(p) = \sum_{n,m} H_{n,m} f_n^*(p) f_m(p) \quad (3.34)$$

and

$$\Gamma_{(k_s, k_i, p)} = \left[ \frac{f_1^*(p) f_2(p)}{\sum_{n,m} H_{n,m} f_n^*(p) f_m(p)} \right], \quad (3.35)$$

where  $H_{n,m}$  can be expressed in terms of  $F_{n,m}$ ,  $D_n(k_i)$ , and  $D_n(k_s)$  by using equations (3.33) in equation (3.34).

It follows that if  $\Sigma'$  is to be obtained variationally, then the requirement that  $\Sigma'$  is an extremum with respect to  $f_n$  is equivalent to the set of equations

$$\sum_n \left[ H_{n,m} - \frac{1}{\Gamma} \delta_{1,n} \delta_{2,m} \right] f_n = 0, \quad (3.36)$$

which has non-trivial solutions if

$$\det \left\{ H_{n,m} - \frac{1}{\Gamma} \delta_{1,n} \delta_{2,m} \right\} = 0. \quad (3.37)$$

Thus,

$$\Sigma' = - \left[ \frac{\det |M_{1,2}|}{\det |H_{n,m}|} \right], \quad (3.38)$$

where  $\det |M_{1,2}|$  is the cofactor of  $H_{1,2}$ . Note that (3.38) gives  $\Sigma'$ , uniquely, as the ratio of two determinants for a particular value of  $p$ , for which  $p_{||}$  [component of  $p$  parallel to the crystal surface] is fixed by the Bethe condition leaving  $p_z$  [component of  $p$  perpendicular to the crystal surface] free. This result (3.38) is valid for the one-Bloch-wave trial function.

As indicated earlier,  $p_z$  is to be treated as a variational parameter.

There are two distinct cases:

(i) When  $E = k^2$  lies in a band, one can find  $p_z$  by setting  $\det |F_{1j,1'j'}| = 0$ . This is done by fixing  $E$  and varying  $p_z$  till the determinant passes through zero because as illustrated by the one-dimensional example, this is equivalent to band structure condition.

(ii) When  $E$  lies in the band gap, procedure (i) will not yield a zero to the determinant. Actually,  $p_z$  is to be taken as complex. This is equivalent to the case of  $E < V_0$  for one-dimensional example. It is essentially a method of finding  $E$  versus  $p$  relation when  $p$  is complex.

### 3.8 Discussion :

The formalism presented here clearly shows the extent to which the variational treatment can be carried out and the simplification that can be achieved with it. It also shows the intimate connection between the band theory, i.e., the KKR method of band structure calculation and the LEED intensity calculation. This fact is very helpful in view of the computational facilities available for the electronic structure calculations.

That no physical aspect of the problem is lost because of the approximations involved in the formalism can be seen by a comparison with the work of Watts<sup>4</sup> which is based on multiple scattering theory. Thus the expression for intensity contains the  $\delta$ -function sums over reciprocal lattice vectors and the Bethe condition follows as a consequence of the periodicity of the system parallel to the crystal surface in both the approaches, that of Watts and ours. The KKR type matrix elements also appear in the intensity expression of Watts. But our intensity expression involving exact KKR<sup>1,2</sup> matrix elements is more easy for actual calculation compared to his result.

If we consider the computational aspect of the problem, the present formulation is not a complicated one. We have shown that it is possible to express the intensity uniquely as a ratio of two determinants [see expression (3.38)]. The size of these determinants depends upon the number of terms in the trial function [given by (3.24)]. For low energy electrons, this number is certainly small and so is the size of the determinants. And if the symmetry of the problem is exploited fully, as has been done here by using lattice harmonics, the size of the determinants reduces further. Since the elements of the determinants in (3.38) are expressed in terms of exact KKR matrix elements, the numerical computation of the intensity would not pose any problem once the KKR band structure programme is ready. The advantage of this variational calculation is that it avoids matching at the boundary and the detailed calculation of wave field inside the crystal.

Of course, the limitations of the approach come from the use of an approximate trial function [a single-Bloch-wave approximation], and a real static potential [i.e., exclusion of inelastic effects] of the muffin-tin form. This treatment is employed in the next chapter to compute the (0,0) intensity of normally incident electron beam, where we will compare our results with some other theoretical and experimental data and discuss the results.

## CHAPTER IV

### LEED SPECTRUM AND BAND STRUCTURE OF ALUMINIUM

The formalism developed in the last chapter is applied here to compute the (0,0) intensity from (100) surface of Aluminium crystal. In the following section, we formulate the case of normal incidence and back scattering for which immense simplification occurs. Next, we describe our results for the high-energy band structure of Aluminium, and at the end the results are discussed.

#### 4.1 Formulation:

For the case of normal incidence, we take the incident beam of electrons to be perpendicular to the crystal surface, and treat this as the z-direction. Then

$$\underline{k}_i \equiv (0, 0, k), \quad (4.1)$$

$$\theta_i = \phi_i = 0 \quad \text{and} \quad \underline{k}_{i\parallel} = 0.$$

Now, we proceed to find out back-scattering-intensity;

Here

$$\underline{k}_{s\parallel} = 0, \quad (4.2)$$

and hence

$$\underline{k}_{s\downarrow} = k = k_z.$$

Thus in this case we have

$$\begin{aligned} D_{1j}(\underline{k}_i) &= 4\pi R_1(r_i) Q_1(j_1) \sum_{\sigma_{1j}}(0,0) \\ &= D_{1j}(\underline{k}_s), \\ \underline{p} &\equiv (0, 0, p), \end{aligned} \quad (4.3)$$

and the Kohn<sup>30</sup> transformations described by (3.33) do not apply.

However, in this case of  $D_{1j}(\underline{k}_i) = D_{1j}(\underline{k}_s)$ , one can define

$$g_1 = \sum_n D_n(\underline{k}_i) c_n(p) \quad \text{and} \quad (4.4)$$

$$g_n = c_n(p) \quad \text{for } n \neq 1.$$

Then

$$\Gamma = \left[ \frac{g_1^* g_1}{\sum_{n,m} G_{n,m} g_n^* g_m} \right] \quad (4.5)$$

It follows that

$$\sum_n \left[ G_{n,m} - \frac{1}{\Gamma} \delta_{n,1} \delta_{m,1} \right] g_n = 0, \quad (4.6)$$

whence

$$\Gamma(p) = \left[ \frac{\det \begin{vmatrix} m_{1,1} \end{vmatrix}}{\det \begin{vmatrix} G_{n,m} \end{vmatrix}} \right], \quad (4.7)$$

where  $\det \begin{vmatrix} m_{1,1} \end{vmatrix}$  is the minor of  $G_{1,1}$ .

Now to evaluate the elements  $G_{1j,1'j'}$  we note that

$$\sum_{1j,1'j'} F_{1j,1'j'} c_{1j}^*(p) c_{1'j'}(p) = \sum_{1j,1'j'} G_{1j,1'j'} g_{1j}^* g_{1'j'}, \quad (4.8)$$

and using (4.4) one gets

$$\begin{aligned}
 G_{00,00} &= \left[ \frac{F_{00,00}}{(D_{00})^2} \right], \\
 G_{00,1'j'} &= \left[ -\frac{F_{00,00} D_{1'j'}}{(D_{00})^2} + \frac{F_{C0,1'j'}}{D_{00}} \right], \\
 G_{1j,00} &= \left[ -\frac{F_{00,00} D_{1j}}{(D_{00})^2} + \frac{F_{1j,00}}{D_{00}} \right], \\
 G_{1j,1'j'} &= \left[ F_{1j,1'j'} + F_{00,00} \frac{D_{1j} D_{1'j'}}{(D_{00})^2} - F_{00,1'j'} \frac{D_{1j}}{D_{00}} \right. \\
 &\quad \left. - F_{1j,00} \frac{D_{1'j'}}{D_{00}} \right], \quad \begin{cases} 1,1' \neq 0 \\ j,j' \neq 0 \end{cases} \quad \dots(4.9)
 \end{aligned}$$

Now, substituting from (2.18) and (4.3) in (4.9), and after doing some algebra, we get

$$\Gamma(p) = \left[ 16 \lambda^2 M_{00}^2(0,0) \right] \left[ \frac{\det \{m'\}}{\det \{G_{1j,1'j'}\}} \right], \quad (4.10)$$

where  $\det \{m'\}$  is the minor of  $G_{00,00}'$ . After putting

$$M_{00} = M_{00}(0,0) \quad (4.11)$$

and

$$M_{1j} = M_{1j}(0,0),$$

the elements  $G_{1j,1'j'}'$  are given by:

$$G_{00,00}' = \lambda_{00,00},$$

$$G_{00,1'j'}' = [\lambda_{00,1'j'} M_{00} - \lambda_{00,00} M_{1'j'}],$$

$$G'_{1j,00} = \left[ \lambda_{1j,00} Y_{00} - \lambda_{00,00} Y_{1j} \right],$$

and  $G'_{1j,1'j'} = \left[ \begin{array}{l} \lambda_{1j,1'j'} Y_{00} Y_{00} + \lambda_{00,00} Y_{1j} Y_{1'j'} \\ - \lambda_{1j,00} Y_{00} Y_{1'j'} - \lambda_{00,1'j'} Y_{00} Y_{1j} \end{array} \right] \begin{array}{l} , \\ , \\ , \\ , \end{array} \begin{array}{l} 1,1' \neq 0 \\ j,j' \neq 0 \end{array} \right].$

... (4.12)

#### 4.2 Band Structure Calculations:

It is already mentioned, that the knowledge of the real and complex band structure of a crystal is required before taking up the intensity calculations. The KKR method of band structure calculation is adopted to compute the electronic structure of aluminium. The choice is aluminium, because lot of experimental information is available for it.

For the energy  $E$  in the band gap, the electron wave vector  $\underline{p}$  is taken as complex. Then one specifies  $E$  within the band gap and solves for the real and imaginary parts of  $\underline{p}$  as function of  $E$ . For complex  $\underline{p}$ , the Bethe condition stays, but structure factors and structure constants get changed. The expressions for structure constants obtained by Kohn-Rostoker<sup>2</sup> are no longer useful for complex  $\underline{p}$  case. In that case, one has to evaluate the structure constants ab initio. Kerre-Phariseau<sup>5</sup> have derived explicit expressions for structure constants, when  $\underline{p}$  becomes complex.

There are a variety of problems, like LEED intensity calculations, which need to probe the electronic states of a solid well above the Fermi

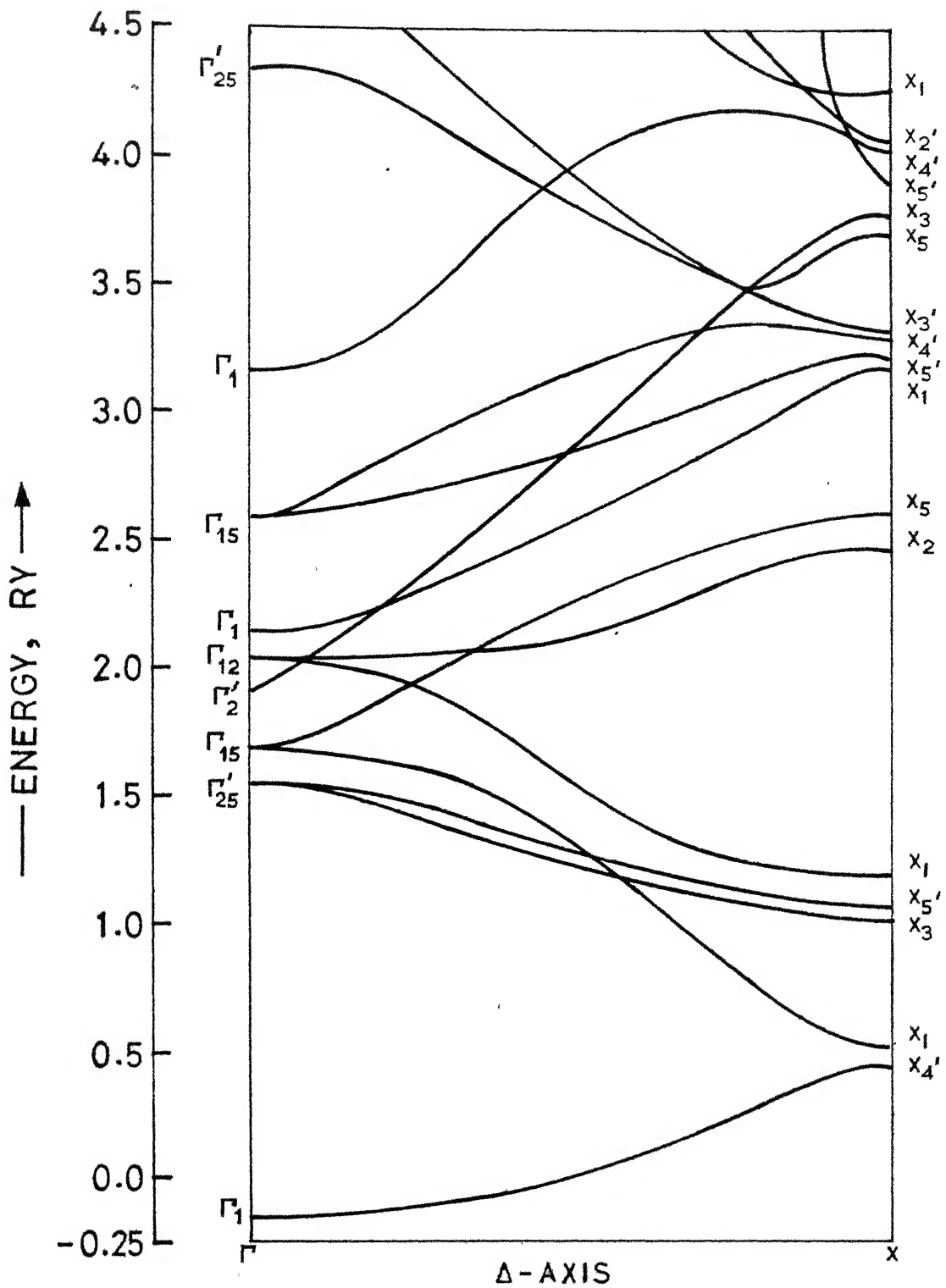


FIGURE 1: ENERGY BAND STRUCTURE OF AL  
ALONG  $\Delta$ -AXIS

level [i.e., high-energy band structure of a solid]. Figure 1 shows our results for high-energy band structure of aluminium along the symmetry direction,  $\Delta$ . Only few other calculations of the high energy band structure of aluminium have been performed by Connolly<sup>31</sup> [self-consistent APW calculation], Hoffstein-Boudreaux<sup>32</sup> [OPW based pseudo-potential calculation], and recently by Jepsen et al.<sup>7</sup> [from eigenvalues of transfer matrix].

Self-consistent potential for aluminium obtained by Snow<sup>33</sup> is employed. The programme was tested for and found to give the well-known rapid convergence of KKR method. We also used Mathieu potential and found that the results of Ham-Segall<sup>9</sup> are reproduced. The programme has been found satisfactory for the range of energy involved in LEED intensity calculations. The results in both low and high energy region are in fair agreement with the previously published data. In low energy region the results emphasize the free-electron like nature of aluminium.

The energy bands also have been compared with the calculations by Connolly<sup>31</sup> and Jepsen et al.<sup>7</sup> with the same potential<sup>33</sup> for aluminium. Careful comparison shows that but for a few discrepancies in limited regions the results are very close. It is important to point out that any residual inaccuracy is unlikely to affect the variational calculation of the LEED intensity.

#### 4.3 Results and Discussion:

Ultimate justification of any variational calculation lies in the quality of the final results. In this spirit we have computed the (0,0)

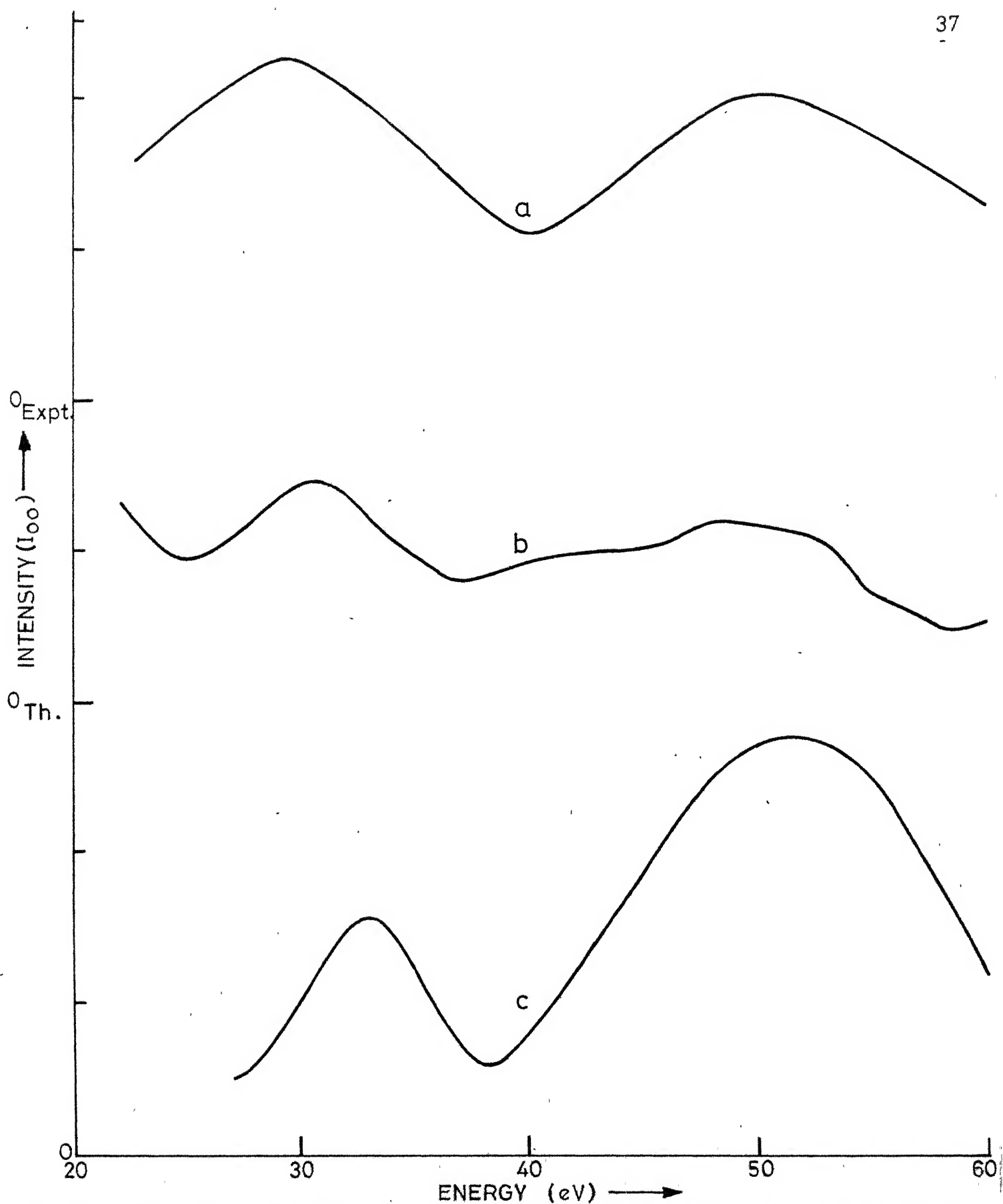


FIGURE 2: COMPARISON BETWEEN MEASURED AND CALCULATED BEAM INTENSITIES VERSUS ENERGY FOR THE (0,0) BEAM FROM THE (100) SURFACE OF Al, NORMAL INCIDENCE. THE ZEROS FOR CURVES a,b,c MARKED WITH  $^0_{\text{Expt.}}$ ,  $^0_{\text{Th.}}$ ,  $^0$ ; RESPECTIVELY.

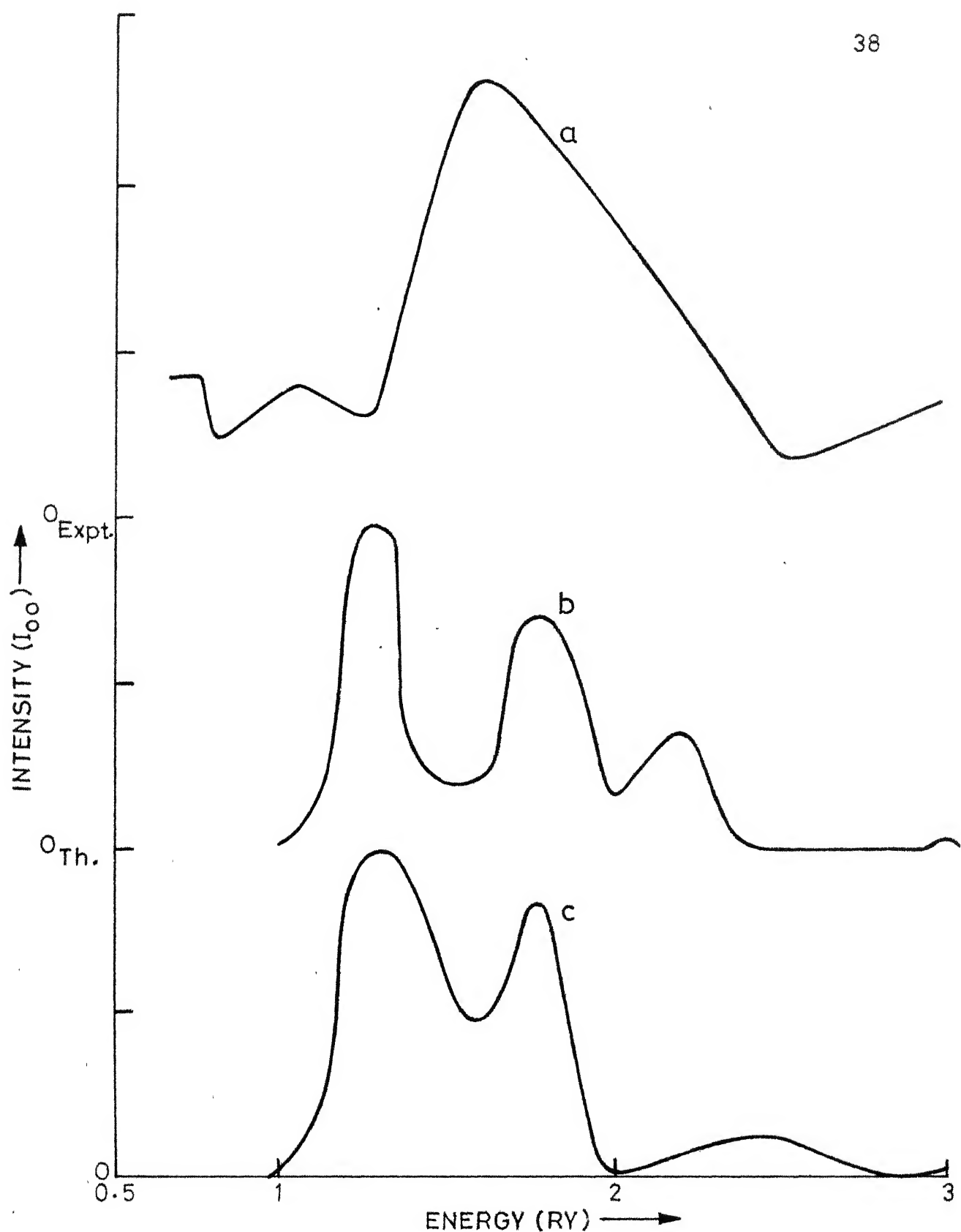


FIGURE 3: COMPARISON BETWEEN MEASURED AND CALCULATED BEAM INTENSITIES VERSUS ENERGY FOR THE (0,0)BEAM FROM THE (100) SURFACE OF AI, NORMAL INCIDENCE. THE ZEROS FOR CUVES a,b,c MARKED WITH  $O_{\text{Expt.}}$ ,  $O_{\text{th.}}$ ,  $O_c$ ; RESPECTIVELY.

intensity from (100) surface of Al for normal incidence, as a test case. The Figs. 2 and 3 compare our results with some other experimental and theoretical results. In both the figures, the curves "a" are experimental<sup>34,35</sup> curves, the curves "b" are obtained from band-matching calculations,<sup>29,36</sup> and the curves "c" are the computed results from our variational formulation. We have included, in these calculations, only the first few  $l$  values in view of the rapid convergence in  $l$  that one gets for the KKR method. The accompanying high-energy band structure calculation of Al by KKR method justifies this convergence for the energy range involved in the present calculation. The contribution estimated for higher  $l$  values is very small and may be ignored for the present purpose.

While comparing the above curves one must keep in mind that our model is a gross simplification of the experimental situation of LEED and that the reproduction of the fine structure, exact peak heights and widths of the measured LEED intensity curves has proved to be an extremely difficult task even for the most elaborate computation. Therefore, ignoring such "fine" effects, there is a great similarity between the experimental curves and the calculated curves. Our results in Fig. 2 are better than those from band matching calculations with a "Single-Bloch-Wave-Approximation"<sup>29</sup> while in Fig. 3 they are comparable with Hoffstein-Boudreaux<sup>36</sup> calculations. With the possibility of numerous other physical realities being brought into the calculation, such an agreement is remarkable and provides ample justification for the chosen trial wave function.

## CHAPTER V

### ELECTRONIC STRUCTURES OF BERYLLIUM AND TITANIUM

#### 5.1 Introduction:

Electronic structures of Beryllium and Titanium, the two typical hexagonal close-packed [hcp] metals, are of considerable theoretical and experimental interest. In literature, there exist theoretical calculations<sup>37,38</sup> of their band structures using methods other than the Green's function method. We report, in this chapter, our theoretical results<sup>39</sup> on electronic band structure of Beryllium and Titanium obtained by employing the Green's function method.

As already mentioned earlier, the Green's function method deserves wide application. But the method has found application mostly to cubic<sup>10</sup> metals and limited application to other structures.<sup>11</sup> There are two reasons for this, namely, the computational difficulties encountered while computing the band structure of complex crystals and the inadequacy of the muffin-tin approximation in case of structures which are not cubic. However, the case of the hcp metals is different, because for the hcp metals the muffin-tin approximation is almost as good as for the cubic metals. It is also possible to simplify the computation to a great extent by the careful application of group-theoretical factorization<sup>13</sup>

of the secular determinant. Then it is interesting to apply the Green's function method to compute the band structure of the hcp metals and fully exploit its virtue of fast convergence of eigenvalues. This has been a major consideration of the present study which also provides useful information for comparison with the results by other methods.

Beryllium, the lightest of all the hcp metals, has a simple atomic configuration  $(1s)^2, (2s)^2$ . Its band structure is very well known and the first theoretical band structure calculation<sup>40</sup> was done as early as in 1940. For the present study, its serves as a test case. On the other hand, the band structure of Titanium has been studied rather recently.<sup>38</sup> It is a typical transition metal with more accepted atomic configuration  $(3d)^2, (4s)^2$ . In view of the limited experimental information and a few theoretical calculations, its band structure needs to be investigated further. The Green's function method is a valuable tool to carry out such investigations. The results are expected to exhibit the general features of the hcp transition metals.

## 5.2 Brief Account of the Method:

Green's function method for "complex" crystals was developed by Segall,<sup>12</sup> in a manner parallel to that of the Kohn-Rostoker<sup>2</sup> method for "simple" crystals. In this section, we give just an outline of the method<sup>12</sup> and describe the group-theoretical factorization<sup>13</sup> of the secular determinant employing hexagonal harmonics<sup>41</sup> for symmetry points and symmetry directions of the Brillouin zone. The details of the method have been discussed at length in the literature.<sup>12</sup> Here we omit any such detailed discussion.

The complex crystal is defined by the lattice translation vectors,  $\underline{r}_s$ , given by  $\underline{r}_s = n_1 \underline{a}_1 + n_2 \underline{a}_2 + n_3 \underline{a}_3$  [ $n_i = 0, \pm 1, \pm 2, \dots$ ], where  $\underline{a}_1$ ,  $\underline{a}_2$  and  $\underline{a}_3$  are the basis vectors of the lattice; and the set of vectors  $\underline{t}_1, \underline{t}_2, \dots, \underline{t}_v$  which locate the centres of  $v$  atoms in the unit cell. Variational principle as in (2.11) is set up and a procedure very similar to the one by Kohn-Rostoker<sup>2</sup> for the simple crystals is followed to solve the problem of band structure calculation for the complex crystals. The important difference between the two procedures<sup>2,12</sup> is that the quantity  $\Delta$  for the complex crystals [See (2.12)] contains terms with two types of products of surface integrals unlike the case of simple crystals. The first type of products arise from integrals over surfaces centred about the same ion [terms to be called "diagonal" in the centres], and the second type of products are due to integrals over surfaces centred about different ions [terms to be called "off-diagonal" in the centres]. This is a result of having more than one atom per unit cell in the complex crystals. The terms off-diagonal in the centres are slightly more troublesome to evaluate because the natural coordinate systems for the position vectors  $\underline{r}$  and  $\underline{r}'$  in the muffin-tin spheres centred about two different ions have their origin at different points. But after redefining the position vectors and the structural Green's function the off-diagonal terms are readily evaluated. Thus, the quantity becomes the sum of all diagonal and off-diagonal terms. Finally, simplifying the whole thing one arrives at the band structure condition

$$\det \left| \Delta_{lm, l'm'} \right| = 0, \quad (5.1)$$

where

$$\Delta_{lm, l'm'} = \left[ A_{lm, l'm'}^{(\nu, \nu')} + k \int_{1l} \delta_{mm'} \delta_{\nu \nu'} \frac{Q_1(\eta_1)}{Q_1(j_1)} \right]_{r=r_1}. \quad (5.2)$$

The expression,  $\frac{Q_1(\eta_1)}{Q_1(j_1)} \Big|_{r=r_1}$ , is evaluated at  $r = r_1$ , the muffin-tin radius of the  $\nu^{\text{th}}$  sphere in the unit cell. Structure constants  $A_{lm, l'm'}^{(\nu, \nu')}$ , which are diagonal in the centres, are identical to the structure constants  $A_{lm, l'm'}^{(\nu, \nu)}$  in Kohn-Rostoker<sup>2</sup> treatment for a simple crystal with the same translational symmetry. Whereas the structure constants off-diagonal in the centres,  $A_{lm, l'm'}^{(\nu, \nu')}, (\nu \neq \nu')$ , are different.<sup>12</sup> They are discussed in details by Segall.<sup>12</sup>

The secular equation (5.1), while being valid for all  $k$  [crystal momentum vector] vectors including those with special symmetry, can be considerably simplified at symmetry points and along symmetry axes as follows:

Consider simple lattices with only one atom per unit cell for which the trial wave function within the muffin-tin spheres is given by

$$\psi_k(r) = \sum_{l,m} C_{lm} R_l(r) Y_{lm}(\theta, \phi), \quad (5.3)$$

where  $R_l(r)$  radial solution of the Schrödinger equation,  $Y_{lm}(\theta, \phi)$  are the spherical harmonics and  $C_{lm}$  are variational coefficients. One can use symmetry-adapted functions

$$Y_{lj}(\theta, \phi) = \sum_m V_{1,m}^{*j} Y_{lm}(\theta, \phi), \quad (5.4)$$

by determining the coefficients  $V_{1,m}^{*j}$  of the unitary matrix  $V^*$  group-theoretically. Using these functions,  $Y_{lj}(\theta, \phi)$ , one obtains the

secular determinant  $\lambda_{l_j, l'_j}$ , which can be related to  $\Lambda_{l_m, l'_m}$ , obtained by using  $Y_{l_m}(\theta, \phi)$  through the relation

$$\lambda_{l_j, l'_j} = \sum_{m, m'} v_{l, m}^j \Lambda_{l_m, l'_m} v_{l', m'}^{*j},$$

whence

(5.5)

$$\lambda = V \Lambda V^t.$$

As is well known,  $\lambda$  will be in the factorized form [or block diagonal form]. Extending the same idea to the case of hcp structures with two atoms per unit cell, one can easily factorize the determinant. Now the trial wave function can be written as

$$\psi_k(r) = \sum_{l, m} \left[ C_{l m} R_l(r) Y_{l m}(\theta, \phi) + \bar{C}_{l m} \bar{R}_l(\bar{r}) \bar{Y}_{l m}(\bar{\theta}, \bar{\phi}) \right], \quad (5.6)$$

where quantities with bars at the top refer to the second atom in the unit cell as the origin. Again the symmetry-adapted hexagonal harmonics<sup>41</sup> may be used to affect factorization. It is important to point out that if hexagonal harmonics are used directly in the expansion of  $\psi_k(r)$ , one gets involved with two-centred integrals which are very conveniently avoided by using the corresponding transformation matrix  $V$ . Thus, the factorization using  $V$ , which is trivial in the case of one atom per unit cell is very helpful for computation involving more than one atom per unit cell.

### 5.3 Description of the Calculation:

The crystal potentials used for determining the energy eigenvalues are derived by Terrell<sup>37</sup> for Beryllium and Hygh-Welch<sup>38</sup> for Titanium.

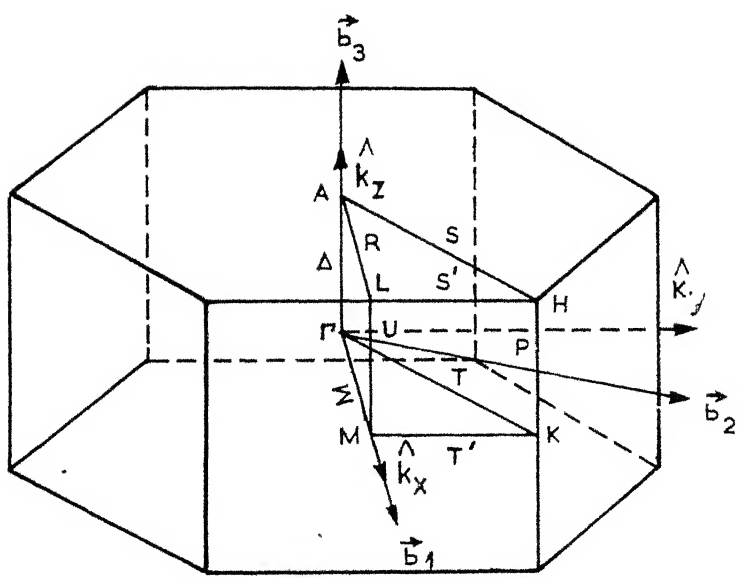


FIGURE 4: THE B.Z. FOR THE HCP CRYSTAL  
WITH THE 1/24 ZONE AND CRYSTAL  
SYMMETRY DIRECTIONS.

TABLE I: Points of 1/24 of the Brillouin zone where energy eigenvalues are computed [Wave vector  $\underline{k} = 2\pi \left[ \left( \frac{\alpha}{24} \right) \vec{b}_1 + \left( \frac{\beta}{24} \right) \vec{b}_2 + \left( \frac{\gamma}{24} \right) \vec{b}_3 \right]$ , where  $\vec{b}_1 = \left( \frac{2}{\sqrt{3}a} \right) \hat{k}_x$ ,  $\vec{b}_2 = \frac{1}{a} \left( \frac{1}{\sqrt{3}} \hat{k}_x + \hat{k}_y \right)$  and  $\vec{b}_3 = \frac{1}{c} \hat{k}_z$  are basis vectors of the reciprocal lattice with  $a$  and  $c$  as the lattice constants.  $\hat{k}_x$ ,  $\hat{k}_y$  and  $\hat{k}_z$  are unit vectors along  $x$ ,  $y$  and  $z$  directions, respectively].

Label	Weightage Factor (No. of like vectors)	Wave Vector ( $\alpha$ , $\beta$ , $\gamma$ )
$\Gamma$	1	(0,0,0)
$\Sigma$	6	(3,0,0)
$\Sigma'$	6	(6,0,0)
$\Sigma''$	6	(9,0,0)
M	3	(12,0,0)
T	6	(2,2,0)
-	12	(5,2,0)
-	12	(8,2,0)
T'	6	(11,2,0)
T	6	(4,4,0)
-	12	(7,4,0)
T'	6	(10,4,0)
T	6	(6,6,0)
T'	6	(9,6,0)
K	2	(8,8,0)
$\Delta$	2	(0,0,6)
-	12	(3,0,6)

TABLE I (..Contd.)

Label	Weightage Factor (No. of like vectors)	Wave Vector ( $\alpha, \beta, \gamma$ )
-	12	(6,0,6)
-	12	(9,0,6)
U	6	(12,0,6)
-	12	(2,2,6)
-	24	(5,2,6)
-	24	(8,2,6)
-	12	(11,2,6)
-	12	(4,4,6)
-	24	(7,4,6)
-	12	(10,4,6)
-	12	(6,6,6)
-	12	(9,6,6)
P	4	(8,8,6)
A	1	(0,0,12)
R	6	(3,0,12)
R	6	(6,0,12)
R	6	(9,0,12)
L	3	(12,0,12)
S	6	(2,2,12)
-	12	(5,2,12)
-	12	(8,2,12)
S'	6	(11,2,12)

TABLE I (..Contd.)

Label	Weightage Factor (No. of like vectors)	Wave Vector ( $\alpha$ , $\beta$ , $\gamma$ )
S	6	(4,4,12)
-	12	(7,4,12)
S'	6	(10,4,12)
S	6	(6,6,12)
S'	6	(9,6,12)
H	2	(8,8,12)

These potentials were calculated by superposing the self-consistent Hartree-Fock atomic potentials and introducing the exchange by means of Slator's free-electron exchange approximation. Apart from the fact that these potentials are satisfactory and carefully constructed, our reasons for using them is also to ease the comparison of the resultant electronic structure.

Figure 4 shows the Brillouin zone for the hcp crystal along with the (1/24) of the zone used in the calculation and the various points and axes of symmetry. The hcp metals contain two atoms in the unit cell so that one has to compute off-diagonal structure constants<sup>12,9</sup> which are, in general, complex. Energy eigenvalues are computed at 45 points in (1/24) of the Brillouin zone. The coordinates of these points along with their weightage factors are given in Table I. Using the symmetry-adapted hexagonal-harmonics<sup>41</sup> up to l=2 we obtained reasonable convergence of eigenvalues.

The Fermi energies,  $E_F$ , are obtained by using the graphically interpolated energy eigenvalues which are equivalent to 1152 points in the Brillouin zone, as follows: There are four electrons per unit cell for Beryllium and eight electrons per unit cell for Titanium and each band can accommodate two electrons per cell. Thus, for a discrete mesh of 1152 points, there will be 2304 energies below Fermi energy for Beryllium and 4608 energies below Fermi energy for Titanium. Arranging the 2304 energies for Beryllium and 4608 energies for Titanium in ascending order and counting up to the 2304<sup>th</sup> energy for Beryllium and 4608<sup>th</sup> energy for Titanium yields the corresponding Fermi energies.

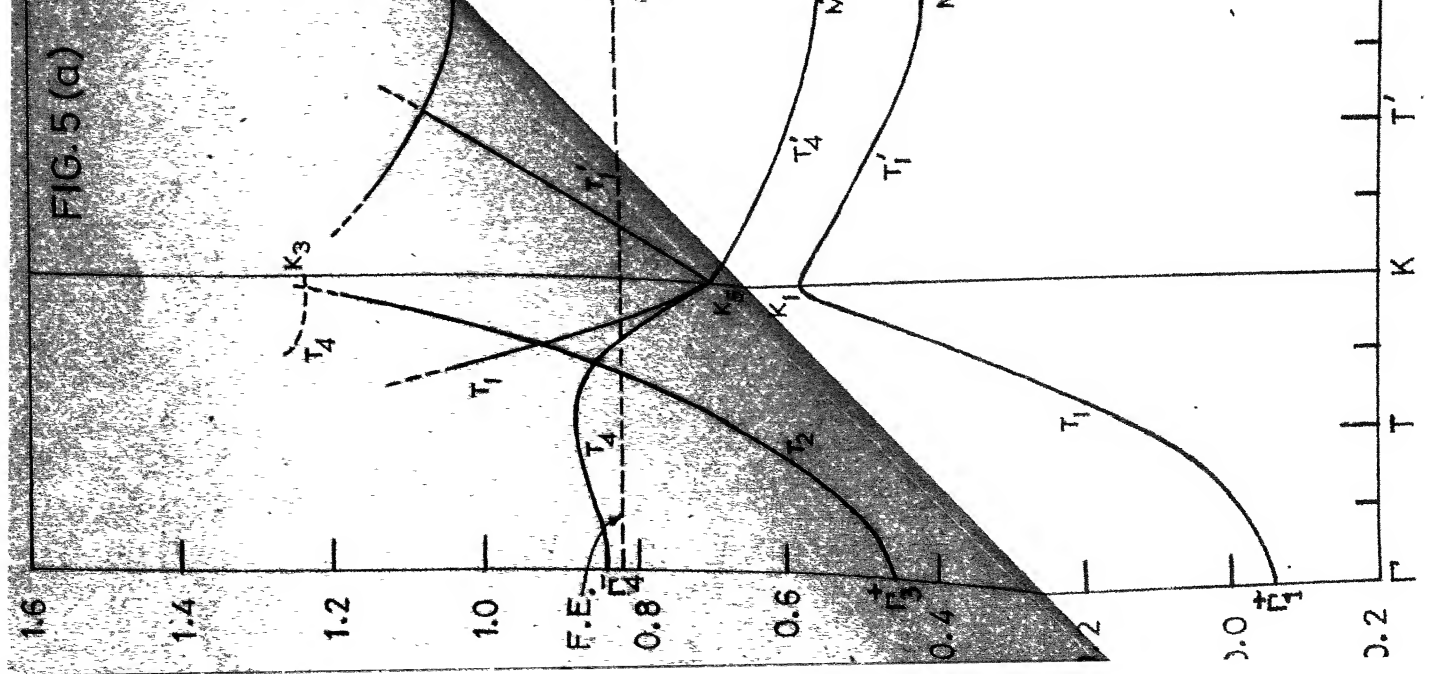


FIG. 5 (a)

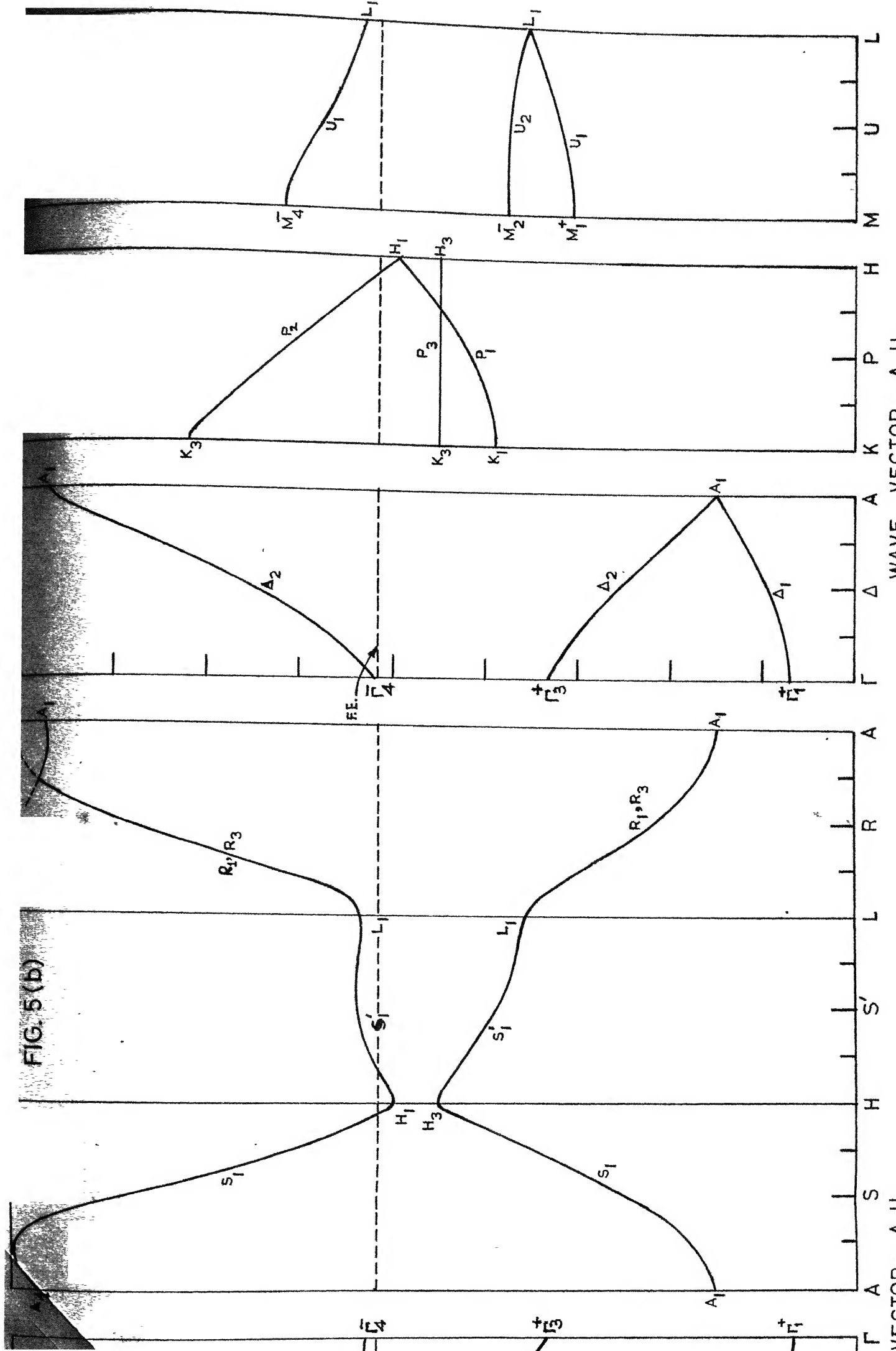


FIGURE 5: THE ENERGY BANDS OF BERYLLIUM ALONG SYMMETRY DIRECTIONS. ALL LEVELS IN (b) DOUBLY DEGENERATE.

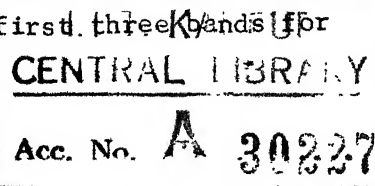
The counting scheme, mentioned above, is also used to calculate the density of states histograms. This is carried out simply by counting the number of the ordered energy eigenvalues that fall within each of a fixed set of energy intervals which cover the calculated energy range. A number of histograms are constructed by varying the energy interval or bar width,  $\Delta E$ , up to the stability situation when no appreciable change takes place in the histogram due to a small alteration in  $\Delta E$ .

For Titanium, the following study is also carried out at a preliminary level. First, the band structure of Titanium is calculated for a value of the exchange parameter,  $\alpha$ , lying in the range of 2/3 to 3/4. This is interesting because it was concluded from an earlier work<sup>38</sup> that  $2/3 \leq \alpha \leq 3/4$  is the possible range of the exchange parameter that could produce results close to reality. Next, the effect of varying the atomic configuration on the band structure of Titanium is studied. This is interesting from the point of view of proper interpretation of experimental information available regarding the band structure and it is closely related to the well known inherent ambiguity for transition metals. In both the cases, the crystal potential was constructed by superposing the self-consistent Hartree-Fock potentials, and the exchange was treated in the Slater's free-electron exchange approximation.

#### 5.4 Results and Discussion:

##### A. Band Structure:

The electronic energy bands for Beryllium along the symmetry directions are shown in Fig. 5. We have shown the first three bands for



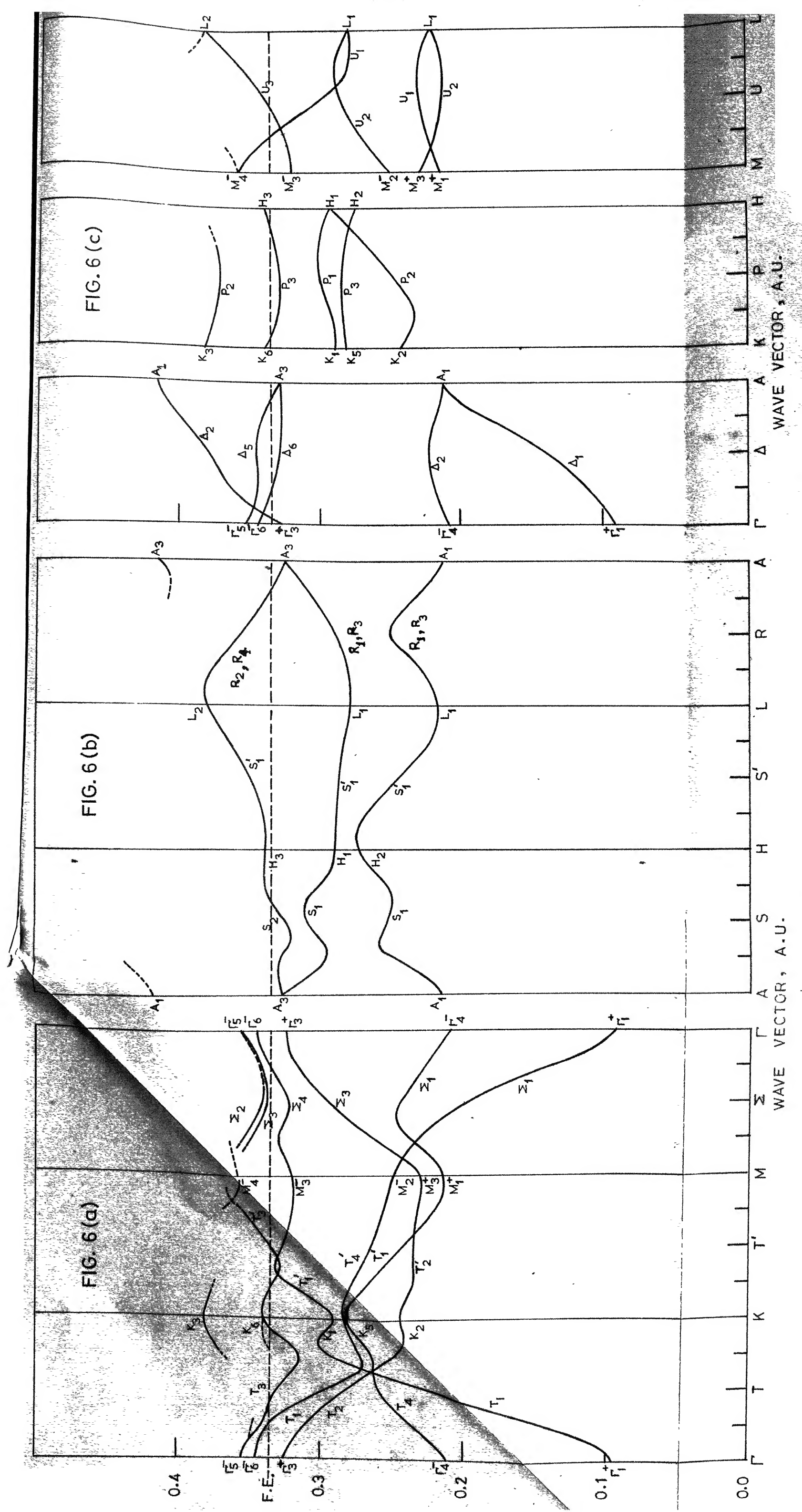


FIGURE 6: THE ENERGY BANDS OF TITANIUM ALONG SYMMETRY DIRECTIONS. ALL LEVELS IN (b) ARE DOUBLY DEGENERATE.

TABLE II. Bandwidths

Be	Occupied Bandwidth, [ $E_F - \Gamma_1^+$ ], in Rydberg.	Ti	Occupied Bandwidth, [ $E_F - \Gamma_1^+$ ], in Rydberg.
<b>Theoretical:</b>			<b>Theoretical:</b>
Herring-Hill <sup>40</sup>	0.865	Hygh-Welch <sup>38</sup>	
Jacques <sup>42</sup>		APW	0.211
Single OPW	0.956	Self-consistent APW	0.153
OPW with variational Parameter	0.919	Present	0.240
APW	0.840	<b>Experimental:</b>	
Cornwell <sup>43</sup>	0.780	Skinner et al. <sup>46</sup>	0.441 (6 eV)
Loucks-Cutler <sup>44</sup>	0.901		
Terrell <sup>37</sup>	0.84 ± 0.01		
Present	0.868		
<b>Experimental:</b>			
Skinner <sup>45</sup>	1.01 ± 0.07		

Beryllium. Since there are four atoms per unit cell and each band is doubly degenerate, on the average there will be two filled bands for Beryllium. The band structure of Titanium along the symmetry directions are shown in Fig. 6. There are eight atoms per unit cell in this case and on the average there will be four filled bands out of the first five bands depicted in Fig. 6.

A comparison between our results and those of Terrell<sup>37</sup> by the Augmented Plane Wave [APW] method for the case of the Beryllium shows a great deal of similarity. Since the electronic structure of Beryllium is well understood, this shows that the present application of the Green's function method has proved to be sound in this test case. Now a comparison of the results of Fig. 6 with those of Hygh-Welch<sup>38</sup> [ APW calculation ] shows that they are very similar.

#### B. Fermi Energy, $E_F$ :

Fermi energies are obtained in both the cases by the counting scheme described in the previous section. We obtain  $E_F = 0.83$  Rydberg for Beryllium and  $E_F = 0.335$  Rydberg for Titanium. Table II compares our results with other theoretical<sup>37,38,40,42-44</sup> and experimental<sup>45,46</sup> results. While our results are very close to those obtained by the APW method in both the cases, the experimental results are significantly different. As usual, a consideration of the difficulties inherent in the extrapolation of the low-energy tail of the x-ray spectra leads to the conclusion that the departure of experimental values from the theoretical values is primarily due to this extrapolation. The limited Fermi surface information derivable from the present calculation indicates

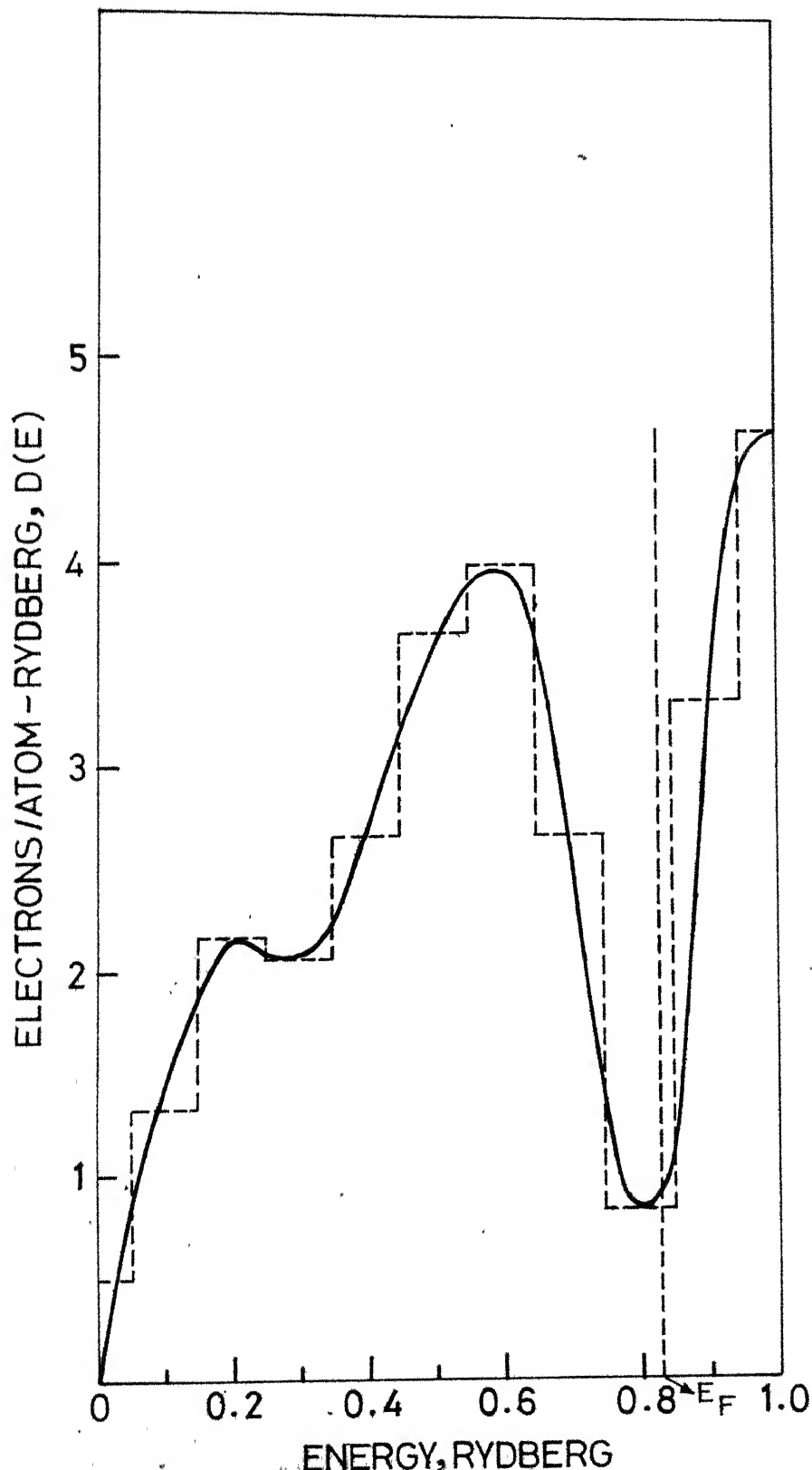


FIGURE 7: DENSITY OF STATES FOR BERYLLIUM

no significant departure from the corresponding APW work which had been rather exhaustive in this respect.

### C. Density of States, D(E):

The density of states histograms are obtained by following the procedure outlined in section 5.3. The resulting stable histograms for Beryllium are obtained for  $\Delta E = 0.1$  Rydberg and is shown in Fig. 7. It resembles very closely with that obtained by Terrell<sup>37</sup>. The basic feature of the density of states curves remain the same in the work of Herring-Hill,<sup>40</sup> Loucks-Cutler,<sup>44</sup> Terrell,<sup>37</sup> and the present calculation.<sup>39</sup>

It is also interesting to point out that the density of states curve for Beryllium shown in Fig. 7 is consistent with the observation of Johnston and Tomboulian,<sup>47</sup> that the x-ray absorption edge coincides with the high-energy limit of the emission line in Beryllium and that the absorption data have a peak at the low-energy end. However, an extension of the density of states calculation to a higher energy is necessary for further comparison with the x-ray data of Johnston-Tomboulian.<sup>47</sup>

The deep minimum in the density of states curve for divalent elements like Beryllium is not the characteristic of the hexagonal structure. But this deep minimum has special relevance in the case of Beryllium because its metallic properties depend upon the overlapping between s and p bands. The band up to Fermi energy represents  $(2s)^2$  electrons of the Beryllium atom and the density of states of course goes to zero in the gaps between energy bands. It is clear from all

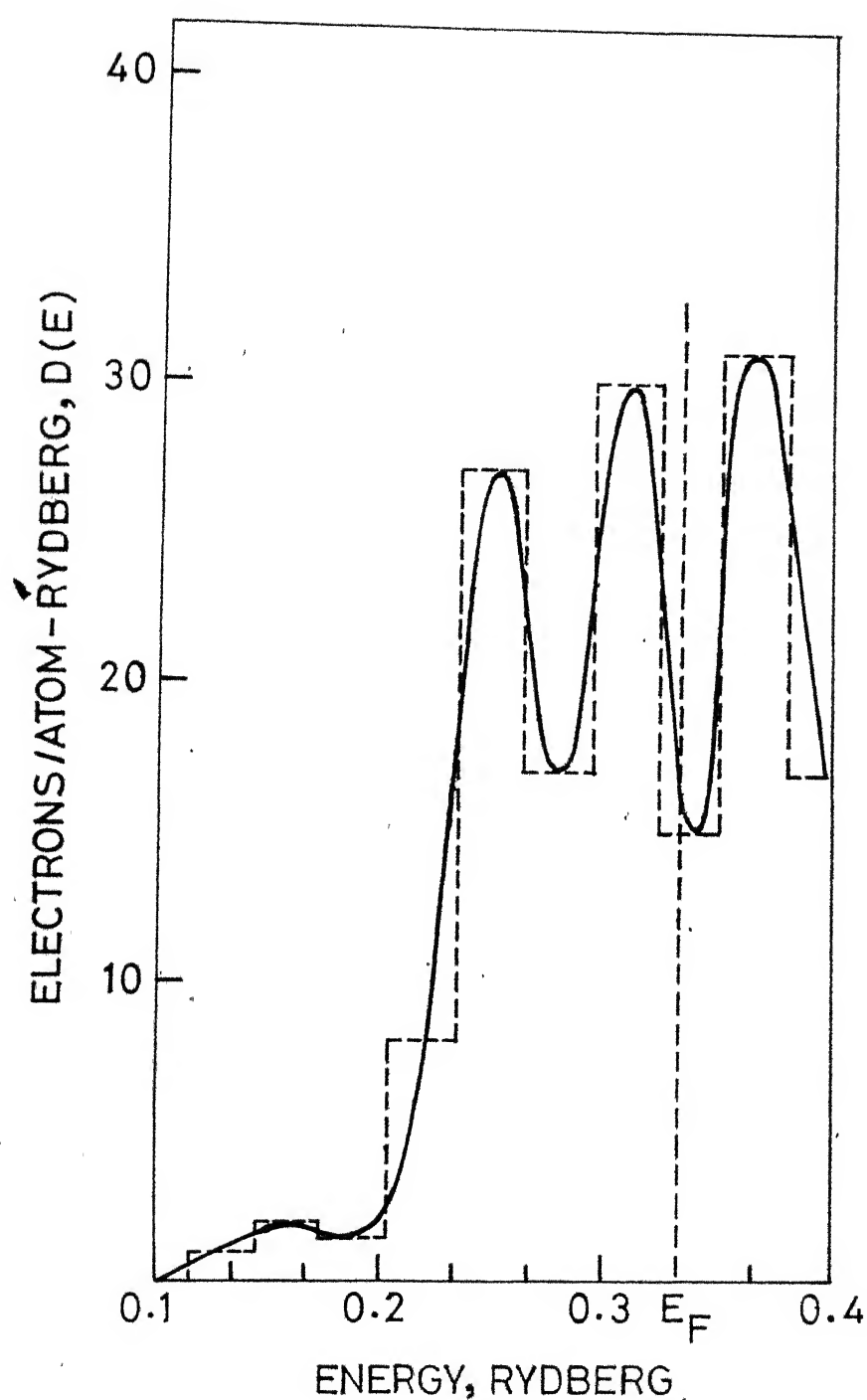


FIGURE 8: DENSITY OF STATES FOR TITANIUM

TABLE III. Heat Capacities

Be	Electronic Specific Heat Coefficient, $\gamma$ , in units of Cal.mole $^{-1}$ deg. $^{-2}$	Ti	Electronic Specific Heat Coefficient, $\gamma$ , in units of Cal. mole $^{-1}$ deg. $^{-2}$
<b>Theoretical:</b>			<b>Theoretical:</b>
Terrell <sup>37</sup>	$0.3 \times 10^{-4}$ to $0.5 \times 10^{-4}$	Hygh-Welch <sup>38</sup>	
Present	$0.41 \times 10^{-4}$	APW	$11.81 \times 10^{-4}$
			Present
			$7.263 \times 10^{-4}$
			Hygh-Welch <sup>38</sup>
			Self-consistent APW
			$9.18 \times 10^{-4}$
<b>Experimental:</b>			<b>Experimental:</b>
Hill-Smith <sup>48</sup>	$0.54 \times 10^{-4}$	Daunt <sup>50</sup>	$8 \times 10^{-4}$
Gmelin <sup>49</sup>	$(0.44 \pm 0.04) \times 10^{-4}$	Gschneider <sup>51</sup>	$7.223 \times 10^{-4}$

this that the deep minimum shows in a graphic way how the overlapping of the (2s) and the (2p) band is not really very great.

The typical density of states curve for hcp metals is exhibited by Titanium as shown in Fig. 8. The histogram agrees well with the one obtained by the APW method.<sup>38</sup> There are two peaks due to the relatively narrow d bands with the Fermi energy on the high-energy side of a relatively sharp minimum.

Theoretical estimate for low temperature electronic specific heat coefficient,  $\gamma$ , is calculated by determining the density of states at Fermi energy  $D(E_F)$ . Our results for both Beryllium and Titanium are compared with other theoretical<sup>37,38</sup> and experimental<sup>48-51</sup> results in Table III.

The estimates of  $\gamma$  from the present calculation may be seen to agree fairly well with other theoretical values in Table III. For Titanium the value of  $\gamma$  is much higher than the free electron value of  $1.15 \times 10^{-4}$  cal.mole.<sup>-1</sup> deg.<sup>-2</sup> The d bands are responsible for the increase in the specific heat value from its free electron value. It may be expected that since the electron-phonon interaction has been neglected in such estimates, there will be some discrepancy with the experimental values. This is borne out by the figures presented in Table III. Titanium is seen to have much less effect of electron-phonon interaction than Beryllium which is very light compared to it.

#### D. Atomic Configuration and Exchange Parameter in Titanium:

The reasons for studying the electronic structure of Titanium with

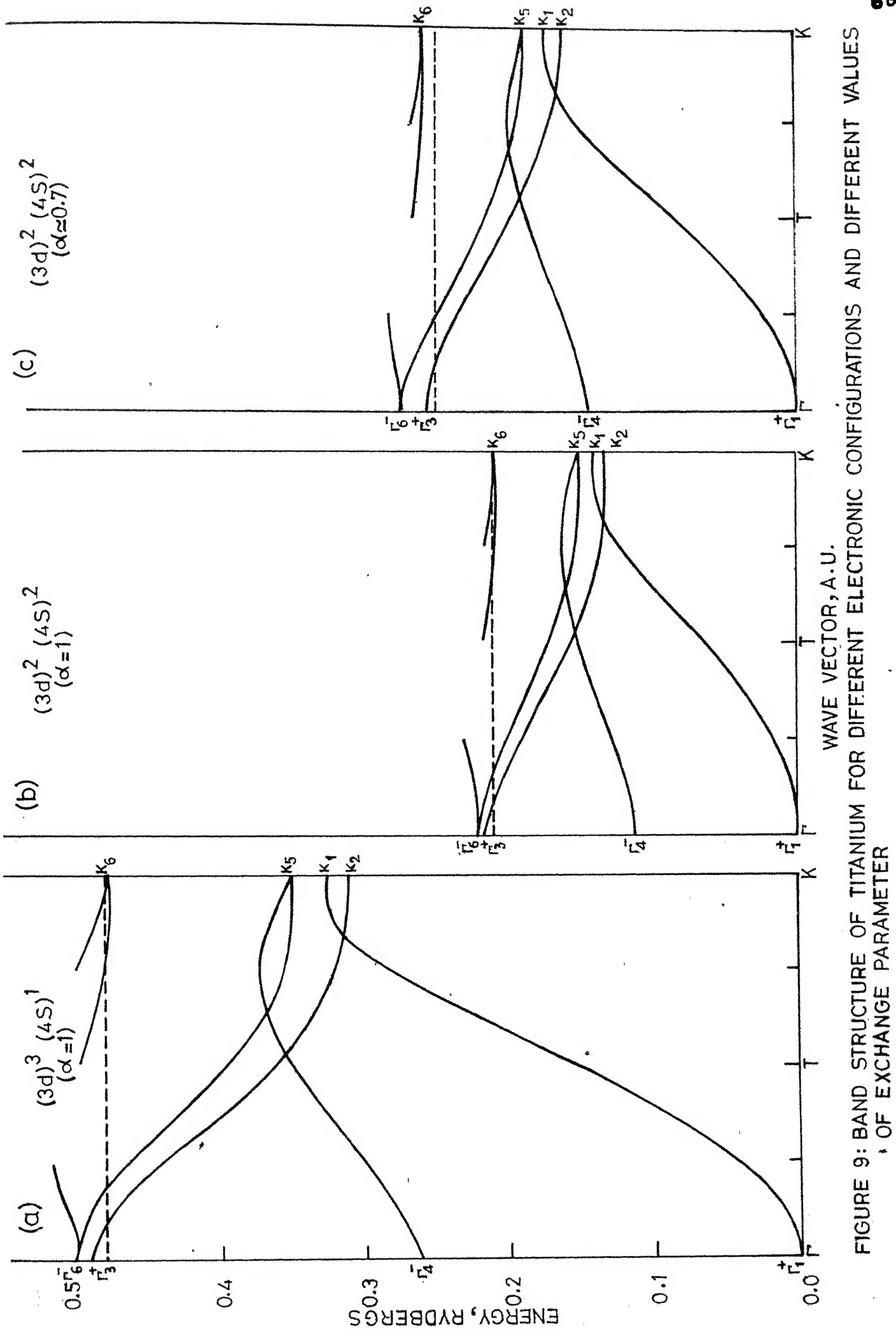


FIGURE 9: BAND STRUCTURE OF TITANIUM FOR DIFFERENT ELECTRONIC CONFIGURATIONS AND DIFFERENT VALUES  
OF EXCHANGE PARAMETER

different atomic configurations and different values of exchange parameter are outlined in the previous section. We have studied these aspects at the preliminary level which is perhaps sufficient to show the qualitative features of the changes that may be expected under these conditions.

The results presented in Fig. 9(a) and Fig. (9b) correspond to the band structure of titanium along  $\Gamma-T-K$  for the atomic configurations  $(3d)^3$ ,  $(4s)^1$  and  $(3d)^2$ ,  $(4s)^2$ ; respectively. Exchange parameter,  $\zeta$ , is taken to be unity in both the cases and the crystal potentials used were obtained by superposing the self-consistent Hartree-Fock atomic potentials with exchange treated in the Slater's free-electron approximation. This kind of variation in the atomic configuration, in general, results in a narrowing of the  $(3d)$  band which is evident from the figure. It is admitted that such computations cannot remove the inherent uncertainty<sup>52,53</sup> of atomic configuration for transition metals. Perhaps the results of self-consistent energy band calculation<sup>38</sup> coupled with detailed and unambiguous experimental information can lead to a satisfactory resolution of the question.

Figure 9(b) and Fig. 9(c) represent band structure of Titanium along  $\Gamma-T-K$  for the atomic configuration  $(3d)^2$ ,  $(4s)^2$  with exchange parameter  $\zeta = 1$  and  $\zeta = 0.7$ , respectively. The second value of  $\zeta = 0.7$  lies in the interesting range of values anticipated from the APW calculation.<sup>38</sup> In Table IV, we show the approximate estimates for occupied band widths  $[E_F - \Gamma_1^+]$  and d band widths  $[\Gamma_6^- - \Gamma_4^-]$  and compare them with other theoretical<sup>38</sup> and experimental<sup>46,54,55</sup> estimates.

This preliminary study indicates that  $\zeta = 0.7$  leads to better agreement with experiment than  $\zeta = 1$ . However, this is no definite conclusion in view of the limited experimental data on Titanium but it surely supports the previous conjecture regarding the interesting range of  $\zeta$ . The exact value of  $\zeta$  will remain an open question for Titanium as long as detailed experimental information is not available.

## CHAPTER VI

### CONCLUSION

Some interesting conclusions, drawn from the present study of "Electron-Diffraction" and "Band Structure" problems by the Green's function method, are as follows.

The variational treatment described in chapter III for the calculation of elastic scattering intensities from a perfect semi-infinite crystal avoids the calculation of cumbersome structure constants by assuming a Bloch wave trial function. The layer-by-layer treatment of the problem appears unnecessary for the case of a perfect semi-infinite crystal. Bethe condition follows, as it should, from the structure factor part of the variational calculation. From the standpoint of computation, it is important to exploit fully the symmetry of the problem. This has been done by using lattice harmonics in the given variational formulation. It has been shown that ultimately the intensity may be found by evaluating the ratio of two very small size determinants which immensely simplifies the computation. And, it has been concluded that such variational calculation of intensity can be performed as a byproduct of the band structure calculation and this fact is very helpful in view of the detailed computational facilities existing for the latter.

The comparison, in Chapter IV, of the computed intensity profiles with the experimentally observed spectra implies that, in practice, one can use the approximate variational treatment given in Chapter III and evaluate elastic LEED intensity curves which can agree within a few per cent with the experimental results. Of course, there are other elaborate computational schemes which lead to very good agreement with experiments. But they involve a lot of labour and computer time. It all depends upon whether one [e.g., an experimentalist] can devote much of time and effort for such computations and whether all the detailed fine structures of LEED intensity spectrum are of interest in any particular case. The method of Chapter III is useful when the efforts that can be put on computation are rather limited. It may be a choice of quick and inexpensive calculation leading to approximate results over a time consuming and expensive calculation producing rather accurate results. This is the conclusion that follows from comparison of our results with those of LEED intensity measurements.

The model considered in Chapter III for intensity calculations is a gross simplification of the experimental situation of LEED and to include more realities one has to consider the important effects like inelastic effects, surface effects, etc. But this would mean putting in tremendous efforts on computation.

The results of electronic structure calculation for Beryllium and Titanium by the Green's function method provide an independent first principle check on the previous theoretical calculations, and

such efforts are in accordance with the best traditions in the Band Structure Theory.: This was not required in case of Beryllium for which quite exhaustive information is available. But the same cannot be said about Titanium. In fact, it is a candidate for still further theoretical and experimental investigations. Perhaps several others like Zirconium etc. in the same period as Titanium should also be studied to resolve the questions regarding atomic configurations and exchange parameter values.

Our results of band structure calculation are quite close to APW results. This may stimulate interest for further theoretical and experimental investigations in case of Titanium. The Green's function method could be a handy tool for such further studies. But no doubt that more detailed and reliable experimental information will be needed before unambiguous theoretical answers can be provided for many important questions. This is exactly why our inferences about  $\epsilon \approx 0.7$  for Titanium must remain at the level of a conjecture.

Finally, we conclude that it is possible to obtain satisfactory numerical results for both the electron scattering problem and the electronic structure problem of the hexagonal close-packed metals by employing properly formulated and carefully simplified form of the Green's function method of Korringa-Kohn-Rostoker.

## REFERENCES

1. J. Korringa, *Physica* 13, 392 (1947).
2. W. Kohn and N. Rostoker, *Phys. Rev.* 94, 1111 (1954).
3. K. Kambe, *Z. Naturforsch.* 22A, 322 and 422 (1967); *ibid.*, 23A, 1280 (1968).
4. C. M. K. Watts, *J. Phys. C* 1, 1237 (1968); *ibid.*, 2, 966 (1969).
5. E. Kerre and P. Phariseau, *Physica* 46, 411 (1970).
6. A. P. Shen, *Phys. Rev. B* 3, 4200 (1971).
7. D. W. Jepsen, F. M. Marcus and F. Jona, *Phys. Rev. B* 5, 3933 (1972).
8. V. V. Bhokare and M. Yussouff, *Nuovo Cimento* 16B, 331 (1973).
9. F. S. Ham and B. Segall, *Phys. Rev.* 124, 1786 (1961).
10. See for example, Methods in Computational Physics, edited by B. Alder, S. Fernbach and M. Rotenberg (Academic Press, New York, 1968), Vol. 8, pp. 251-292.
11. See for example, J. Treusch and R. Sandrock, *Phys. Stat. Solidi* 16, 487 (1966) and G. E. Juras, et.al., *Sol. Stat. Comm.* 10, 427 (1972).
12. B. Segall, *Phys. Rev.* 105, 108 (1957); See for example: R. P. Singh, pp. 941-966, Theory of Condensed Matter, Lectures presented at an International Course, October-December 1967, at ICTF Trieste, Vienna, IAEA, 1968.
13. V. V. Bhokare and M. Yussouff, *Lett. Nuovo Cim.* 5, 470 (1972). Our preliminary results for Be and Ti are also reported here.
14. H. Bethe, *Ann. Physik* 87, 55 (1928).
15. D. S. Boudreux and V. Heine, *Surface Sci.* 8, 426 (1967).
16. P. M. Marcus and D. W. Jepsen, *Phys. Rev. Letters* 20, 925 (1968).

17. K. Hirabayashi and Y. Takeishi, *Surface Sci.* 4, 150 (1966).
18. M. Von Laue, *Phys. Rev.* 37, 53 (1931).
19. E. G. MacRae, *Surface Sci.* 11, 479 (1968).
20. C. G. Darwin, *Phil. Mag.* 27, 675 (1914).
21. J. L. Beeby, *J. Phys. C* 1, 82 (1968).
22. C. B. Duke, J. R. Anderson and C. W. Tucker, *Surface Sci.* 19, 117 (1970).
23. S. Y. Tong and T. N. Rhodin, *Phys. Rev. Letters* 26, 711 (1971).
24. D. W. Jepsen, P. M. Marcus and F. Jona, *Phys. Rev. Letters* 26, 1365 (1971).
25. J. B. Pendry, *J. Phys. C* 4, 2514 (1971).
26. P. J. Feibelman, C. B. Duke and A. Bagchi, *Phys. Rev. B* 5, 2436 (1972).
27. A. P. Shen and J. B. Krieger, *Phys. Rev. B* 1, 2500 (1970).
28. Methods in Theoretical Physics, by P. M. Morse and H. Feshback (McGraw-Hill, New York, 1953), pp. 1130-31.
29. F. Hoffmann and H. F. Smith, *Phys. Rev. B* 1, 2811 (1970).
30. W. Kohn, *Phys. Rev.* 74, 1763 (1948).
31. J. W. D. Connolly, *Intern. J. Quantum Chem.* 3S, 807 (1970).
32. V. Hoffstein and D. S. Boudreux, *Phys. Rev. B* 2, 3013 (1970).
33. E. C. Snow, *Phys. Rev.* 158, 683 (1967).
34. S. M. Bedair, Experimental Data plotted in Ref. 29.
35. F. Jona, *IBM J. Res. Develop.* 14, 444 (1970).
36. V. Hoffstein and D. S. Boudreux, *Phys. Rev. Letters* 25, 512 (1970).
37. J. H. Terrell, *Phys. Rev.* 149, 526 (1966).
38. E. H. Hygh and R. M. Welch, *Phys. Rev. B* 1, 2424 (1970); *ibid.*, B4, 4261 (1971).
39. V. V. Bhokare and M. Yussouff, to be published in *Nuovo Cimento B*.

40. C. Herring and A. G. Hill, Phys. Rev. 58, 132 (1940).
41. S. L. Altmann and C. J. Bradley, Rev. Mod. Phys. 37, 33 (1965).
42. R. Jacques, Cashiers Phys. 70, 71 and 72 (1956).
43. J. W. Cornwell, Proc. Roy. Soc. A261, 551 (1961).
44. T. L. Loucks and E. M. Cutler, Phys. Rev. A133, 819 (1964).
45. H. W. B. Skinner, Phil. Trans. Roy. Soc. (Lon.) A239, 95 (1940).
46. H. W. B. Skinner, T. G. Bullen and J. E. Johnston, Phil. Mag. 45, 1070 (1954).
47. R. W. Johnston and D. H. Tomboulian, Phys. Rev. 94, 1585 (1954).
48. P. Hill and R. Smith, Phil. Mag. 44, 636 (1953).
49. M. E. Gmelin, Compt. Rend. 259, 3459 (1954).
50. J. G. Daunt, Progress in Low Temperature Physics (North-Holland, Amsterdam, 1955).
51. K. A. Gschneider, Solid State Phys. 16, 275 (1964).
52. J. Callaway, Phys. Rev. 99, 500 (1955).
53. L. F. Matheiss, Phys. Rev. 134, A970 (1964).
54. D. E. Eastmann, Solid Stat. Comm. 7, 1697 (1969).
55. R. J. Weiss, Phys. Rev. Letters 24, 883 (1970).

## APPENDIX

Assuming the lattice constant to be unity, one can define

$$f(s-s') \equiv \frac{1}{N} G(r-r'+s-s') e^{-ip(s-s')}$$

Then,

$$\begin{aligned} \sum_{s=0}^N \sum_{s'=0}^N f(s-s') &= \sum_{s'=0}^N \sum_{l=-s'}^{N-s'} f(l), \quad l = s-s' \\ &= \sum_{s'=0}^N \sum_{l=0}^{N-s'} f(l) + \sum_{s'=0}^N \sum_{l=-s'}^{-1} f(l) \\ &= \sum_{l=0}^N \sum_{s'=0}^{N-1} f(l) + \sum_{l=-1}^{-N} \sum_{s'=-1}^N f(l) \\ &= \sum_{l=0}^N (N-1+1)f(l) + \sum_{l=-N}^{-1} (N+1+1)f(l) \\ &= \sum_{l=-N}^{+N} Nf(l) + \sum_{l=-N}^{+N} f(l) - \sum_{l=-N}^{+N} |l| f(l). \end{aligned}$$

The second term is obviously of the order of  $1/N$  and can be neglected compared to the first one. The third term is also negligible because

$$G(x-x') = (-i/2k_0) e^{ik_0 \|x-x'\|}$$

so that for large  $|l|$ ,  $f(l) \approx (-i/2k_0) e^{ik_0 \|l\| - ipl}$ .

Therefore,

$$(-i/k_o) \frac{\partial}{\partial k_o} [k_o f(1)] = |1| f(1)$$

and

$$\sum_{l=-N}^{+N} |1| f(1) = (-i/k_o) \frac{\partial}{\partial k_o} \left[ k_o \sum_{l=-N}^{+N} f(1) \right],$$

which is of the order of  $1/N$  of the first term. Thus the desired result follows. In case of three-dimension, x and y direction lattice sums are trivial and exact and the sum in z-direction needs the above-mentioned approximation.